

GASEOUS HYDROGEN EFFECTS ON THE MECHANICAL PROPERTIES OF CARBON AND LOW ALLOY STEELS (U)

P. S. Lam

Savannah River National Laboratory
Materials Science & Technology Directorate

Publication Date: June 2006

UNCLASSIFIED
DOES NOT CONTAIN
UNCLASSIFIED CONTROLLED
NUCLEAR INFORMATION

ADC &
Reviewing
Official: S.L. West / P.L. West

Date: 6/8/2006

Washington Savannah River Company
Savannah River Site
Aiken, SC 29808

This document was prepared in connection with work done under Contract No. DE-AC09-96SR18500 with the U. S. Department of Energy. Distribution authorized to the Department of Energy only; other requests shall be approved by the cognizant DOE Departmental Element.

DISCLAIMER

This report was prepared as an account of work sponsored by an agency of the United States Government. Neither the United States Government nor any agency thereof, nor any of their employees, makes any warranty, express or implied, or assumes any legal liability or responsibility for the accuracy, completeness, or usefulness of any information, apparatus, product, or process disclosed, or represents that its use would not infringe privately owned rights. Reference herein to any specific commercial product, process, or service by trade name, trademark, manufacturer, or otherwise does not necessarily constitute or imply its endorsement, recommendation, or favoring by the United States Government or any agency thereof. The views and opinions of authors expressed herein do not necessarily state or reflect those of the United States Government or any agency thereof.

DOCUMENT: WSRC-TR-2006-00119 Rev. 1
TITLE: Gaseous Hydrogen Effects on the Mechanical Properties of Carbon and Low Alloy Steels (U)

APPROVALS



Poh-Sang Lam, Author
Materials Applications & Process Technology Group
SRNL-MATERIALS SCIENCE & TECHNOLOGY

Date: 6/8/2006



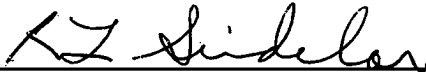
George B. Rawls, Technical Review
Materials Applications & Process Technology Group
SRNL-MATERIALS SCIENCE & TECHNOLOGY

Date: 6/8/2006



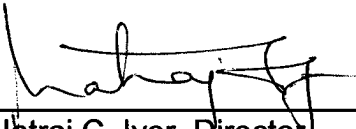
Thad M. Adams, H2 Delivery Program Director
Materials Applications & Process Technology
SRNL-MATERIALS SCIENCE & TECHNOLOGY

Date: 6/8/2006



Robert L. Sindelar, Manager
Materials Applications & Process Technology
SRNL-MATERIALS SCIENCE & TECHNOLOGY

Date: 6/8/2006



Natraj C. Iyer, Director
SRNL-MATERIALS SCIENCE & TECHNOLOGY

Date: 6/8/2006

WSRC-TR-2006-00119 Rev. 1
Table of Contents

EXECUTIVE SUMMARY	1
INTRODUCTION	2
TENSILE PROPERTIES	3
THRESHOLD STRESS INTENSITY FACTOR (K_{th} or K_H)	14
FRACTURE TOUGHNESS	16
FATIGUE CRACK GROWTH	23
CONCLUSIONS	28
REFERENCES	29

List of Tables

Table 1	Tensile ductility data for 0.22% carbon steel (normalized at 900 °C) in hydrogen gas with various pressures [3]	4
Table 2	Un-notched tensile strength in air and in hydrogen [6].....	6
Table 3	Tensile properties for some carbon steels under 10,000 psig of helium and hydrogen [3]	8
Table 4	Unexposed and hydrogen charged tensile properties of a Spanish pipeline material similar to X42.....	12
Table 5	Tensile properties for X42, X70, A516, and A106B in air and in 1000 psi (6.9 MPa) hydrogen gas [12,13].....	14
Table 6	Fracture toughness (J-R curve) for A516 Grade 70 in air and in hydrogen [15] 17	
Table 7	Three-point bend fracture toughness test results for a Spanish line pipe material similar to API X42 under hydrogen pressure (see Figure 14) [11]	19
Table 8	Fracture toughness data determined by burst test for a Spanish line pipe material similar to API X42 under hydrogen pressure (see Figure 14) [11]....	19
Table 9	Fracture toughness (J_{IC} and dJ/da) for X42 and X70 in 6.9 MPa nitrogen and in 6.9 MPa hydrogen [12].....	20
Table 10	Fracture toughness for API 5L Grade B exposed to various pressures of hydrogen [17]	22

List of Figures

Figure 1	Elongation and reduction of area for 0.22% carbon steel in gaseous hydrogen up to 2205 psig (15.2 MPa or 150 atm).	4
Figure 2	The tensile strength of cold-drawn 0.22% carbon steel decreases when the ambient hydrogen pressure increases [5]......	5

Figure 3 The ductility of Armco iron and 0.45% carbon steel decreases when the ambient hydrogen pressure increases [6]. 5

Figure 4 Effect of ductility change as a functions of carbon content for specimens in air (1 atm) and in high pressure hydrogen gas (150 atm), respectively [3]. 6

Figure 5 Comparison of the ductility for carbon steels in 1000 psig helium and in 1000 psig hydrogen..... 7

Figure 6 Metallography of un-notched tensile specimen indicated the formation of cracks in 10,000 psig hydrogen environment [7,3]: (a) Cross-section; (b) crack configurations. 8

Figure 7 Hydrogen lowered the 0.2% yield stresses of the carbon steels (P1: quenched and tempered; P2: controlled rolled at -10 °C) [8]. 9

Figure 8 Hydrogen gas charged (left) and cathodically charged (right) tensile tests show that the yield stresses were increased due to hydrogen in the materials [9]...... 10

Figure 9 Temperature dependent embrittlement index for various materials [9]..... 11

Figure 10 The change of reduction of area as a function of charge current density or hydrogen concentration for a line pipe material similar to X42 [10]. 12

Figure 11 Change in reduction of area as a function of exposing hydrogen pressure for Spanish line pipe materials using double-notched tensile specimens [10,11].13

Figure 12 Threshold stress intensity factors at crack arrest in various hydrogen pressures [14]...... 15

Figure 13 Crack growth resistance (J-R) curves for A516 Grade 70 in Air and in Hydrogen [15]...... 17

Figure 14 Hydrogen pressure-dependent fracture toughness for a Spanish line pipe material similar to API X42 [11]. 18

Figure 15 The crack growth resistance (J-R) curves for X42 base metal in 6.9 MPa (1000 psig) pressure of nitrogen and in 6.9 MPa of hydrogen [12]...... 20

Figure 16 The J-R curves for API 5L Grade B in 13.8 MPa (2000 psi) nitrogen and in 13.8 MPa (2000 psi) hydrogen [17]...... 21

Figure 17 The pressure dependent J_{IC} for API 5L Grade B in hydrogen [17] 22

Figure 18 Fatigue crack growth rates (da/dN) for (a) X42 and (b) X70 in 6.9 MPa (1000 psi) hydrogen and in 6.9 MPa (1000 psi) nitrogen at stress ratio $R= 0.1$ [12]23

Figure 19 Fatigue crack growth rates (da/dN) for X42 in hydrogen and in nitrogen at various stress ratios (R) [12]. 24

Figure 20 Fatigue crack growth rates (da/dN) for as rolled and normalized API 5L Grade B steels in various pressures of hydrogen (1Hz) and in air (10 Hz) [17]. 25

Figure 21 Fatigue crack growth rates (da/dN) for as rolled and normalized API 5L Grade B steels as a function of hydrogen pressure [17] 25

Figure 22 Fatigue crack growth rate for ASME SA-105 Grade II steel exposed to hydrogen up to 15,000 psi under $R=0.1$ and 0.1 Hz cyclic load [20] 26

Figure 23 Cyclic frequency effects on ASME SA-105 Grade II steel in 15,000 psi hydrogen ($R= 0.1$) [20] 27

EXECUTIVE SUMMARY

This report is a compendium of sets of mechanical properties of carbon and low alloy steels following the short-term effects of hydrogen exposure. The property sets include the following:

Yield Strength
Ultimate Tensile Strength
Uniform Elongation
Reduction of Area
Threshold Cracking, K_H or K_{th}
Fracture Toughness (K_{IC} , J_{IC} , and/or J-R Curve)
Fatigue Crack Growth (da/dN)

These properties are drawn from literature sources under a variety of test methods and conditions. However, the collection of literature data is by no means complete, but the diversity of data and dependency of results in test method is sufficient to warrant a design and implementation of a thorough test program. The program would be needed to enable a defensible demonstration of structural integrity of a pressurized hydrogen system. It is essential that the environmental variables be well-defined (e.g., the applicable hydrogen gas pressure range and the test strain rate) and the specimen preparation be realistically consistent (such as the techniques to charge hydrogen and to maintain the hydrogen concentration in the specimens).

INTRODUCTION

An infrastructure of new and existing pipelines and systems will be required to carry and to deliver hydrogen as an alternative energy source under the hydrogen economy. Carbon and low alloy steels of moderate strength are currently used in hydrogen delivery systems as well as in the existing natural gas systems. It is critical to understand the material response of these standard pipeline materials specified by the American Petroleum Institute (API) [1] when they are subject to pressurized gases of pure hydrogen or its mixture with methane since hydrogen is well known in deteriorating the mechanical properties of steels.

A literature survey for existing mechanical property data on carbon and low alloy steels exposed to hydrogen gas was conducted to support the program led by the Concurrent Technologies Corporation for hydrogen pipeline life management. This report documents the data available in the open literature.

In the evaluation of the fitness-for-service for the line pipes used to transport hydrogen gas, the mechanical properties relevant to new construction or extended life of existing systems include the yield stress (σ_y); ultimate tensile strength (UTS); elongation; reduction of area; fracture toughness expressed by the critical stress intensity factor K_{IC} or K_{JC} , J-integral (J), or crack resistance curve (J-R); the stress intensity factor threshold or the stress intensity factor at crack arrest (K_{th}) below which no crack growth in the hydrogen environment is likely; and the fatigue crack growth rate (da/dN , where a is the crack length and N is the number of cycles). The fatigue testing is typically in terms of the difference of the maximum and minimum stress intensity factors or $\Delta K = K_{max} - K_{min}$, and the cyclic stress ratio, $R = K_{min}/K_{max}$.

The change of mechanical properties is caused by the material response to hydrogen. However, the form of exposure or the type of attack directly affects the degradation mechanism in the materials, and results in various, sometimes opposite, effects [2] such as reported on the strain hardening or softening behavior. This report will only document the mechanical property changes due to hydrogen-environmental embrittlement. The embrittlement due to direct chemical interaction between the gaseous hydrogen and the metals, as well as the internal embrittlement related to steel-making process, are out of the scope of the report.

As pointed out by many authors, for example, Jewett et al (1973) [3], the mechanical properties of materials in a hydrogen environment cannot be compared on an equal basis because material composition, strain rate, testing procedure including the hold time prior to testing, sample preparation including charging method, hydrogen pressure and purity, etc. will affect the test results. In general, the change in the elastic properties is insignificant with the presence of hydrogen. However, the deformation capacity (ductility), fracture mechanics properties including fracture toughness and fatigue crack propagation characteristics are deteriorated as the hydrogen pressure increases. Typical test results in the open literature for carbon steels relevant to the pipeline materials are collected and are documented in this report.

In this report, the hydrogen affected tensile properties are first documented, followed by threshold stress intensity factor, the fracture toughness, and the fatigue crack growth data. Information on test pressure, temperature, strain rate, and gas purity are reported as appropriate, and the original work is referenced and is traceable if more detailed information of the experiments is needed. The collection of literature data is by no means complete, but the diversity of data is sufficient to warrant a conclusion that a thorough test program must be implemented. It is essential that the environmental variables be well-defined (particularly, the hydrogen gas pressure range and the strain rate) and the specimen preparation be realistically consistent (such as the hydrogen charge technique and to maintain the hydrogen concentration in the steels). In addition, to facilitate the predictive methodology and the fitness-for-service assessment analyses, the companion tensile testing for the full stress-strain curve should be performed along with the fracture mechanics property testing including fatigue; even the fracture test procedures specified by the American Society for Testing and Materials (ASTM) do not require tensile properties.

TENSILE PROPERTIES

The tensile properties found in the literature typically include one or more of the following: yield stress, ultimate tensile strength, elongation, and reduction of area. They were reported mainly to demonstrate the hydrogen effects at various levels of pressure or concentration. The data may be useful for codified analyses which require strength information of the steels. However, for a realistic structural analysis or fracture performance analysis with the finite element method, in general, a full stress-strain curve beyond linear elasticity up to failure would be required.

A comprehensive mechanical property report on the hydrogen embrittlement effects on various structural alloys including (but not limited to) carbon steels can be found in Reference 3, which is a summary of a research project sponsored by National Aeronautics and Space Administration (NASA) prior to 1973. In the experimental programs for the tensile properties, the researchers used un-notched and notched specimens. The notched specimens provided stress concentration in the gage section so the hydrogen concentration is enhanced locally resulting in a more pronounced effect. However, the test data based on this type of specimens may be inadequate for stress analysis in structural integrity-related issues; rather, they do provide a convenient screening method in selecting the materials of construction. Therefore, in the current report, only the tensile properties derived from un-notched specimens are reported unless otherwise identified.

The earliest tensile test conducted in hydrogen gas up to 2205 psig (15.2 MPa or 150 atm) for 0.22% carbon steel was carried out by Hofmann and Rauls in 1961 [4] as quoted in Reference 3. Their results on tensile ductility are summarized in Table 1 and plotted in Figure 1. Table 1 also provides additional information for this material when the tests

were performed in air and in 1470 psig argon gas (inert environments). The tensile strength of this material in hydrogen was not reported by the original researchers.

Table 1 Tensile ductility data for 0.22% carbon steel (normalized at 900 °C) in hydrogen gas with various pressures [3]

Pressure psig	Pressure atm	UTS ksi	Elongation (gage: 30 mm) %	Reduction of Area %
ambient (Air)	1 (Air)	70.8	32	64
147 (H ₂)	10 (H ₂)		34.5	52
294 (H ₂)	20 (H ₂)		33	47
735 (H ₂)	50 (H ₂)		30	50
1470 (H ₂)	100 (H ₂)		30	36.5
2205 (H ₂)	150 (H ₂)		26	28
1470 (in Argon)	100 (in Argon)		36	62

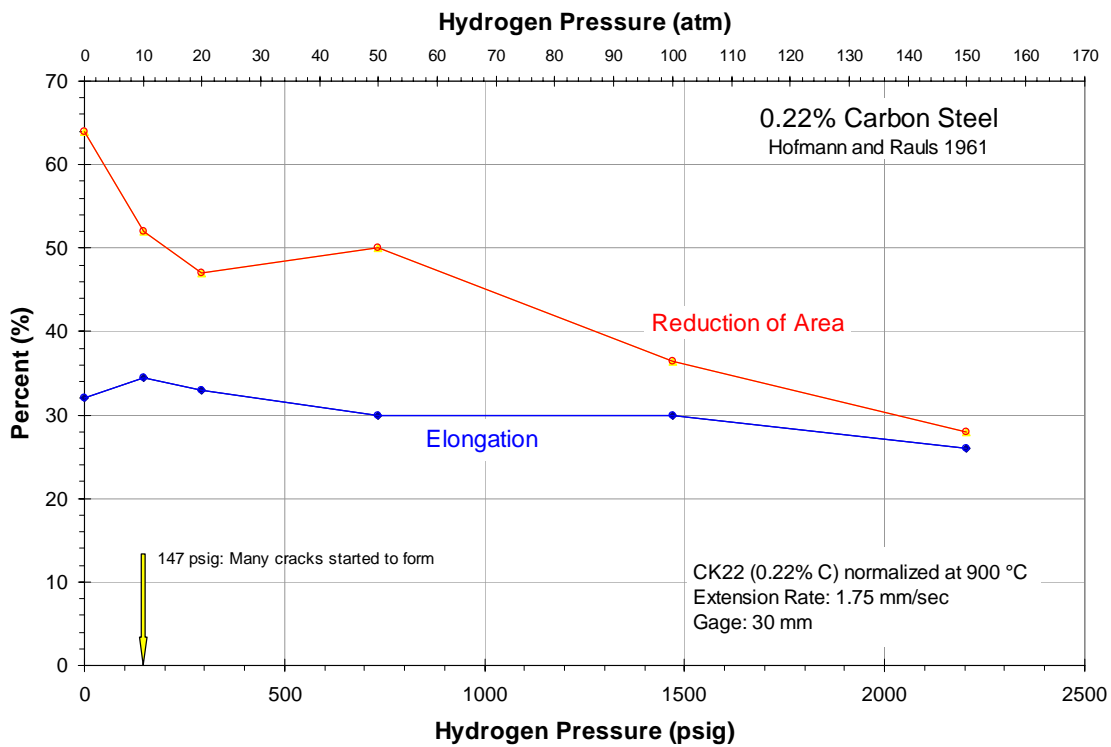


Figure 1 Elongation and reduction of area for 0.22% carbon steel in gaseous hydrogen up to 2205 psig (15.2 MPa or 150 atm).

The cold-drawn 0.22% carbon steel was used in another test, again by Hofmann and Rauls [5]. The lowering of the UTS is shown in Figure 2 (reproduced from Reference 3). The ductility data obtained for Armco iron and 0.45% carbon steel under gaseous hydrogen from 14.7 to 2205 psig were also reported [6] and are replotted in Figure 3.

Both the UTS and the ductility of these carbon steels decrease as the hydrogen pressure increase from 14.7 to 2205 psig. Furthermore, these authors [6] correlated their ductility data in terms of carbon content of the test specimens (Figure 4).

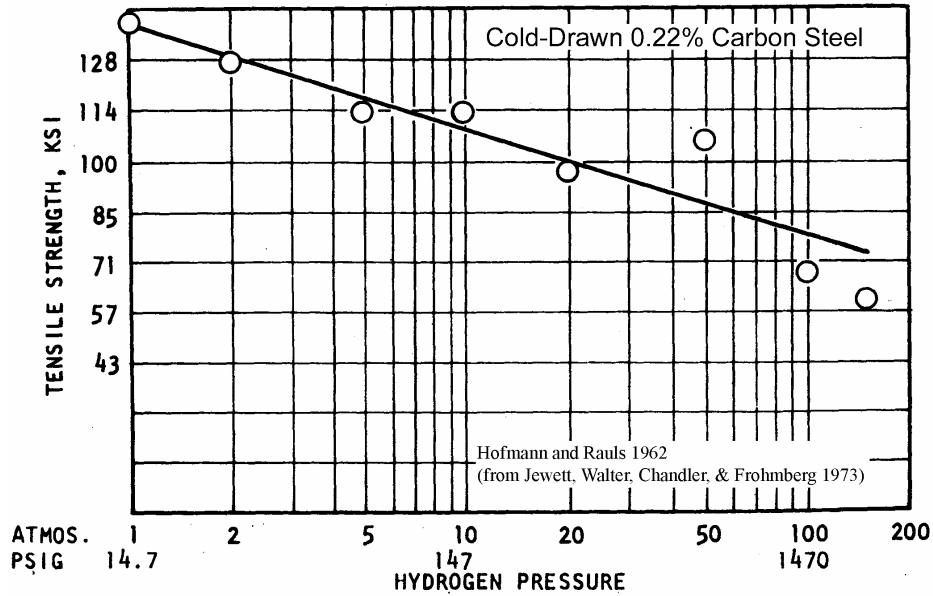


Figure 2 The tensile strength of cold-drawn 0.22% carbon steel decreases when the ambient hydrogen pressure increases [5].

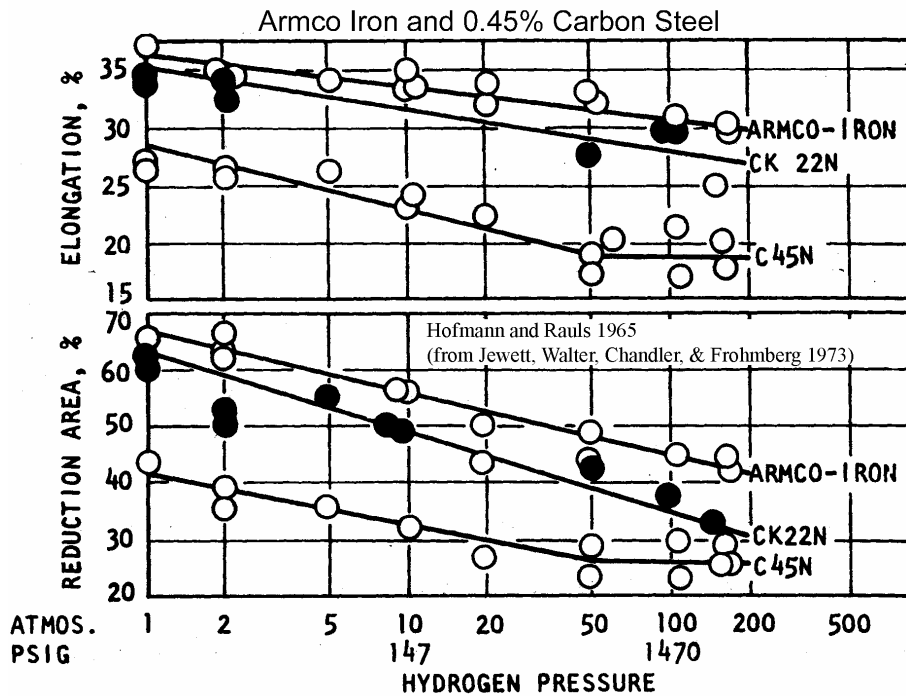


Figure 3 The ductility of Armco iron and 0.45% carbon steel decreases when the ambient hydrogen pressure increases [6].

For the materials in Figure 3, the numerical comparison of UTS in air and in hydrogen is shown in Table 2, in which only the un-notched data were extracted from Table 5 in Reference 3. It is noted that the UTS did not change due to the high pressure hydrogen. However, when the notched specimens were used, a 30% reduction in UTS was observed in 2205 psig hydrogen gas [3,6]. It is believed that the hydrogen concentration was further enhanced near the root of the notch due to stress concentration.

Table 2 Un-notched tensile strength in air and in hydrogen [6]

Material	UTS (ksi)	
	Air	Hydrogen at 2205 psig
Armco Iron	51.4	48.6
0.22% C Normalized	71	71
0.45% C Normalized	96.2	96.2

Figure 4 was reproduced from Reference 3 and shows the dependence of material ductility on the carbon content. It is clear that both elongation and reduction of area are reduced significantly from the values in the air. In this particular case, the hydrogen gas is 2205 psig (15.2 MPa or 150 atm).

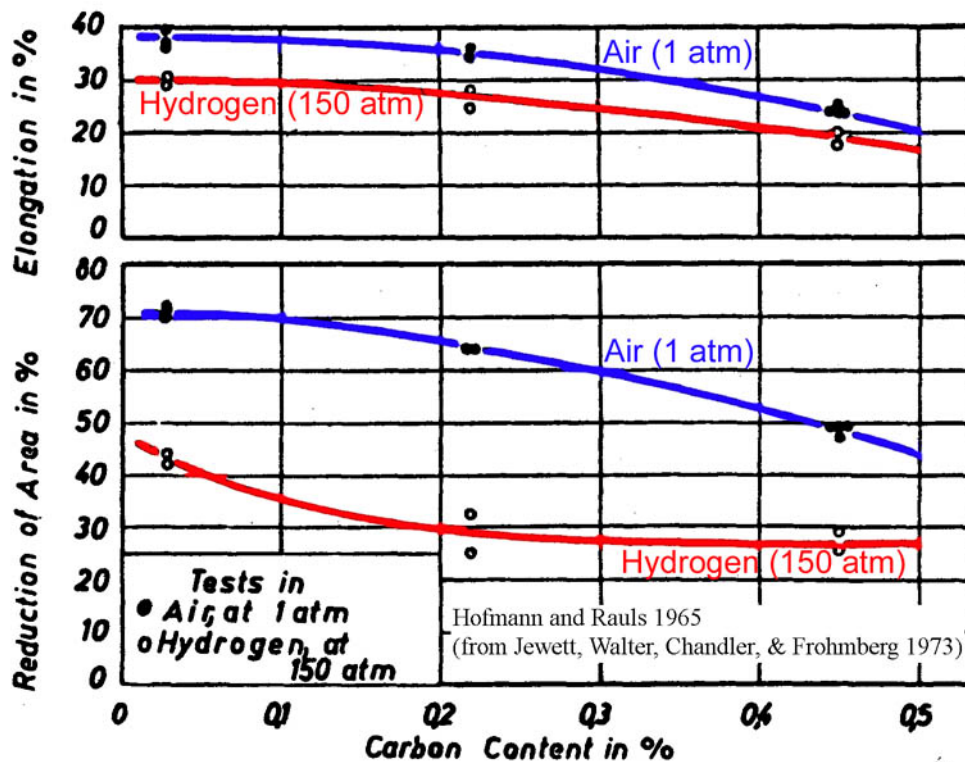


Figure 4 Effect of ductility change as a functions of carbon content for specimens in air (1 atm) and in high pressure hydrogen gas (150 atm), respectively [3].

Table 8 of Reference 3 also lists the tensile test results for 36 iron, nickel, titanium, aluminum, and copper-base alloys in helium (inert environment) and in hydrogen. The pressure range for both gases was from 7000 to 10,000 psig. The yield stress, tensile strength, elongation, and reduction of area were originally reported by Walter and Chandler (1969) [7]. The carbon steels of moderate strength from that investigation include ASTM A-515 Gr. 70, AISI 1042 Normalized, AISI 1020, and Armco Iron. All these materials were subject to 10,000 psig of helium or hydrogen. The elongation and reduction of area from that work are presented graphically in Figure 5 to demonstrate the effect of high pressure hydrogen. However, the yield stress and the UTS were essentially unchanged (the maximum variation is about 2 ksi). These values are listed in Table 3. This finding seems consistent with that reported by Hofmann and Rauls [6] (see Table 2).

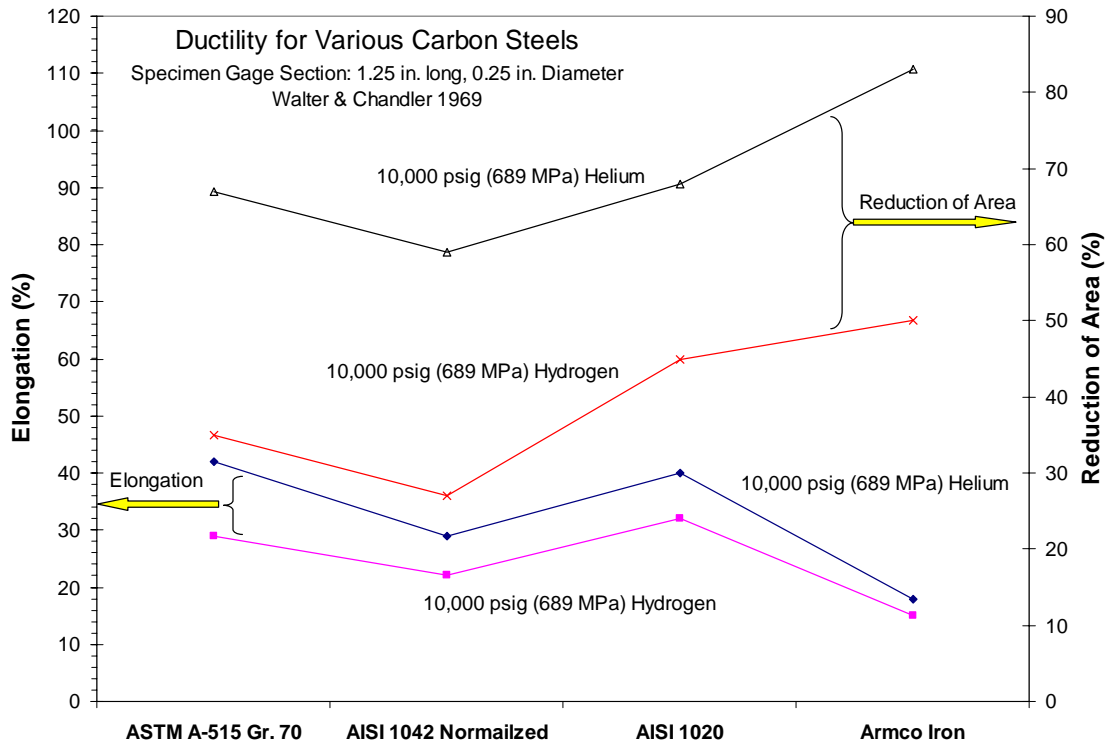


Figure 5 Comparison of the ductility for carbon steels in 1000 psig helium and in 1000 psig hydrogen.

Table 3 Tensile properties for some carbon steels under 10,000 psig of helium and hydrogen [3]

Material	Yield Stress ksi		Tensile Strength ksi		Elongation %		Reduction of Area %	
	He (10,000 psig)	H ₂ (10,000 psig)	He (10,000 psig)	H ₂ (10,000 psig)	He (10,000 psig)	H ₂ (10,000 psig)	He (10,000 psig)	H ₂ (10,000 psig)
ASTM A-515 Gr. 70	45	43	65	64	42	29	67	35
AISI 1042 Normalized	58	NA*	90	89	29	22	59	27
AISI 1020	41	40	63	62	40	32	68	45
Armco Iron	54	NA*	56	57	18	15	83	50

*NA: not available.

Reference 3 also reported that under high pressure hydrogen tensile testing, cracking was initiated on the outside surface of some specimens.

Figure 6 shows the metallography of AISI 1020 specimen in 10,000 psig hydrogen gas tested by Walter and Chandler [7]. Multiple semi-circular cracks were seen to grow inward from the gage area and the crack orientation was perpendicular to the loading direction. Note that the typical composition for AISI 1020 is 0.17-0.24% C, 0.25-0.60% Mn, with the following representative tensile properties in air: minimum yield stress 36 ksi, UTS 58 ksi, elongation 36%, and reduction of area 59%.

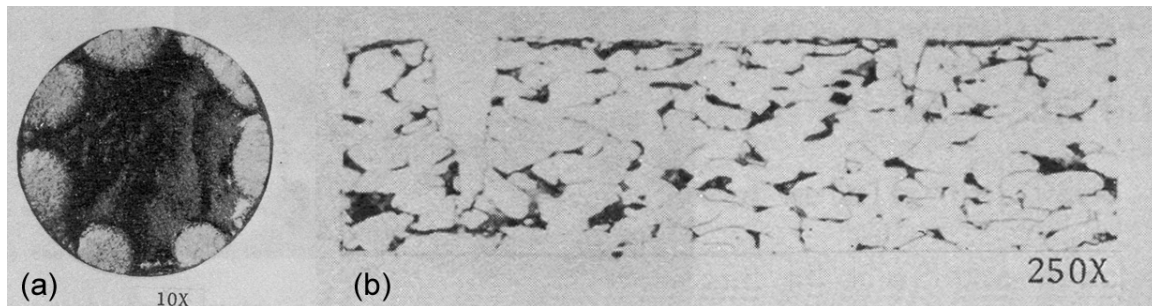


Figure 6 Metallography of un-notched tensile specimen indicated the formation of cracks in 10,000 psig hydrogen environment [7,3]: (a) Cross-section; (b) crack configurations.

Ellis, Bartlett and Knott (1990) [8] used an Amsler 500 ton press to apply various prestrains to steel blanks to modify (increase) the yield stress of the same alloys (P1 and P2, which contained 0.092 and 0.094 wt.% of carbon, respectively). The specimens were then cathodically charged with hydrogen with a thin layer of copper plate deposited onto the surface of the exposed specimen to prevent hydrogen from escaping. Subsequently, the specimens were held for 24 hours at room temperature so the hydrogen could be

distributed uniformly in the specimen. Figure 7 shows that the 0.2% yield stress was reduced by the presence of hydrogen at various prestrain levels (or equivalently, for at various yield stress level) of the alloys. Note that the UTS curves were available in the original work [8], but are deleted from Figure 7 because the data points were ambiguously presented in their published work.

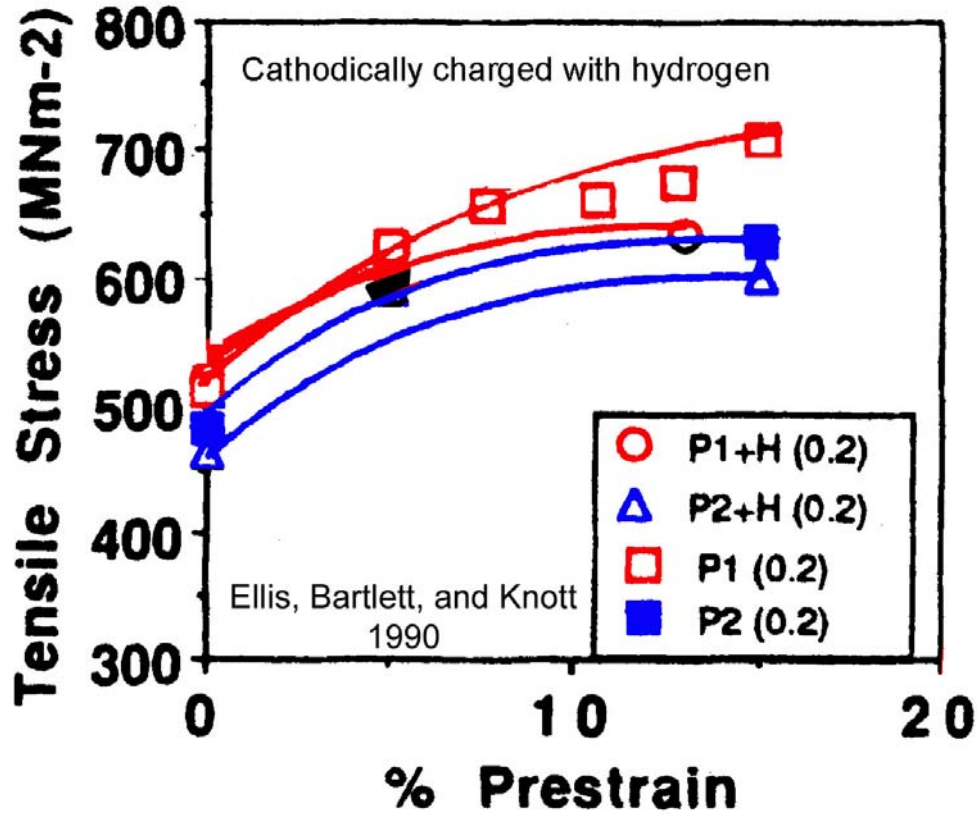


Figure 7 Hydrogen lowered the 0.2% yield stresses of the carbon steels (P1: quenched and tempered; P2: controlled rolled at -10 °C) [8].

In contrast, results from the testing carried out by Pussegoda and Tyson (1981) [9] showed that the hydrogen would raise the flow properties of the materials (Figure 8). This is opposite to the findings of previously discussed results. Two representative sets of results are quoted here: 1) QT specimens (quenched and tempered); and 2) DQ specimens (directly quenched). The QT specimens were charged in hydrogen gas at 650 °C for 3 hours, quenched into an ice water bath, and stored in liquid nitrogen until testing. The hydrogen concentration was about 1 ppm (wt.%). The DQ specimens were cathodically charged in solution at a heated (80 °C) solution to produce a range of hydrogen concentrations from 1 to 5 ppm, and then stored in nitrogen gas until testing. The tensile testing was conducted in a temperature range of -196 to 135 °C. The charged tensile specimens tested above ambient temperature were electroplated with a thin layer of cadmium to prevent offgas.

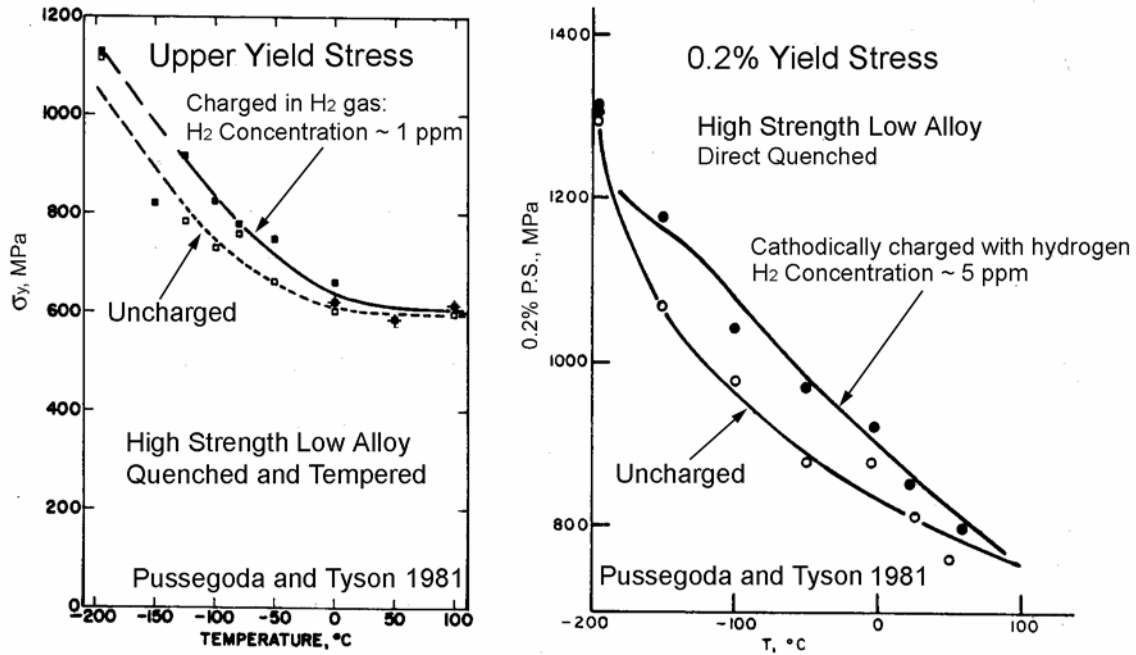


Figure 8 Hydrogen gas charged (left) and cathodically charged (right) tensile tests show that the yield stresses were increased due to hydrogen in the materials [9].

The temperature dependent ductility is expressed as embrittlement index (EI) and is shown in Figure 9 for various materials with different yield stresses. The embrittlement index is defined as

$$EI = (\epsilon_{fu} - \epsilon_{fc}) / \epsilon_{fu}$$

and

$$\epsilon_f = \ln(A_o - A_f)$$

where ϵ_f is the failure strain in the loading direction, A_o is the original cross-sectional area of the tensile specimen, and A_f is the cross-sectional area at failure. The additional subscripts “u” and “c” represent “uncharged” and “charged,” respectively.

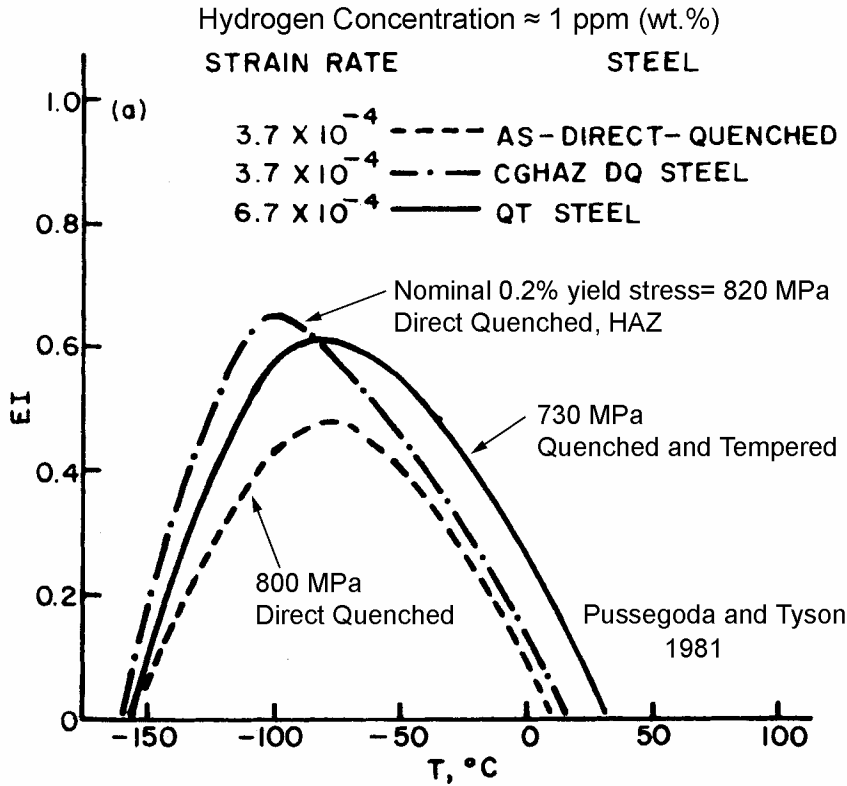


Figure 9 Temperature dependent embrittlement index for various materials [9].

Three types of Spanish line pipe steels were tested by Chritenson et al. (1980) [10]. Their Pipe No. 2, which is similar to X42 steel specified by API [1], was also tested by Gutierrez-Solana and Elices (1982) [11] for fracture toughness. For Pipe No. 2, the smooth tensile specimens were cathodically charged, and immediately tested to minimize hydrogen loss. The unexposed and hydrogen-exposed tensile properties are summarized in Table 4, which shows that the effect of hydrogen on the tensile strength is not pronounced within the range of cathodic charge current densities (or the hydrogen concentration range, see the abscissa in Figure 10). Note that the hydrogen concentration in this work was up to about 40 ppm, which has far exceeded that of 1 to 5 ppm in Figure 8 and Figure 9 by Pussegoda and Tyson [9]. However, significant change in reduction of area was reported: about 80% in the longitudinal direction and about 60% in the transverse direction, as shown in Figure 10. The change in reduction of area is defined as $(RA_u - RA_c) / RA_u$, where RA_u and RA_c are the reduction of areas of the uncharged and charged specimen, respectively.

Table 4 Unexposed and hydrogen charged tensile properties of a Spanish pipeline material similar to X42

Pipe No. 2 (similar to X42)	0.2% Yield Stress (MPa)	UTS (MPa)	Reduction of Area (RA)
Unexposed	266 (Longitudinal)	414 (Longitudinal)	61%
	286 (Transverse)	417 (Transverse)	51%
Cathodically Charged H ₂	294 (Averaged)	424(Averaged)	change up to 80%

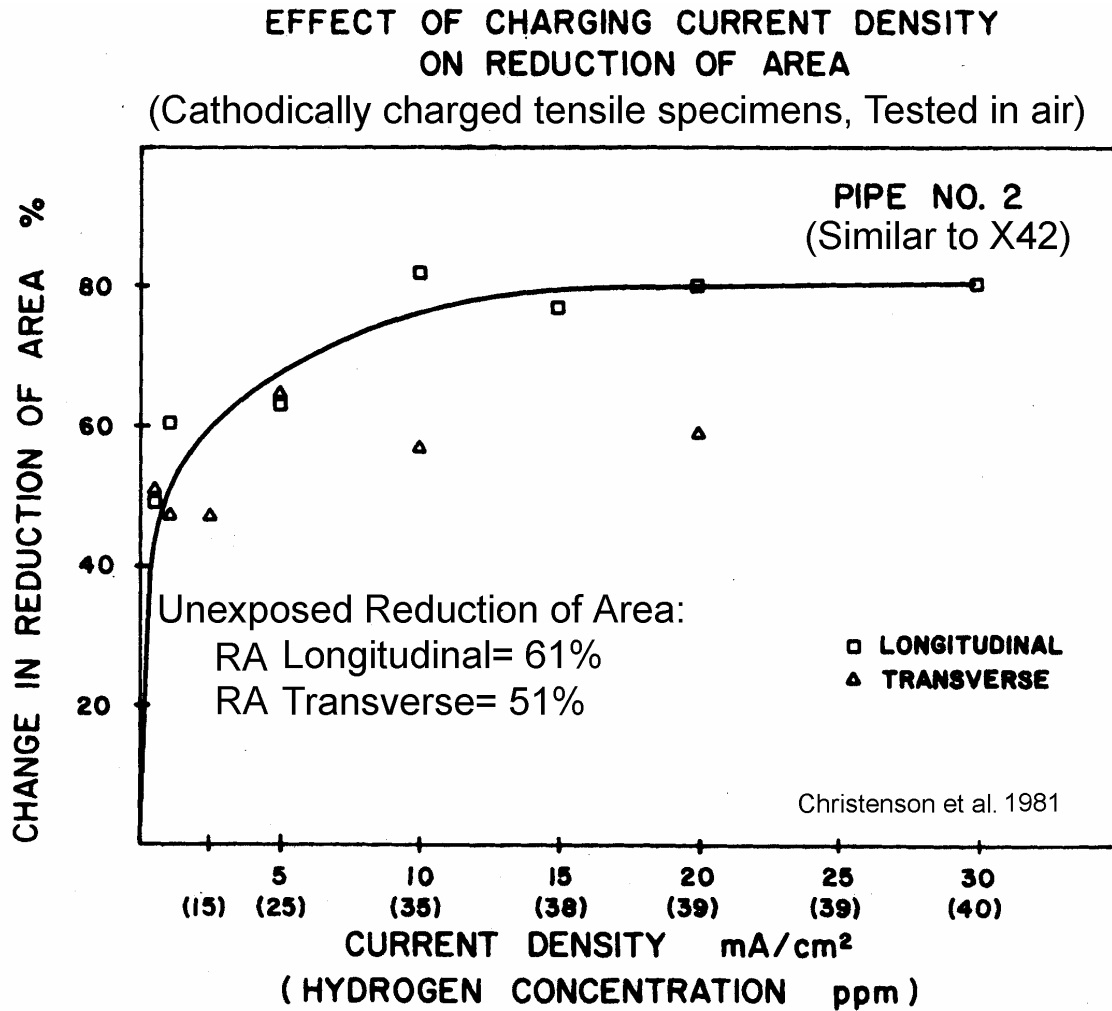


Figure 10 The change of reduction of area as a function of charge current density or hydrogen concentration for a line pipe material similar to X42 [10].

The changes in reduction of area for notched tensile specimens were also tested by Christenson et al. [10] and reported by Gutierrez-Solana and Elices [11]. Included in this test series, additional line pipe materials (Pipe No. 1 and a plate), along with Pipe No. 2 (discussed earlier in the last paragraph) were used [10]. These tensile specimens were double notched, and were tested in pressurized hydrogen atmosphere up to 34.5 MPa

(5000 psi). The resulting changes in reduction of area are plotted as a function of external hydrogen pressure and are shown in Figure 11 (the unexposed reduction of area for these notched specimens are not available). It can be seen from Figure 11 that the reduction of area has been severely deteriorated when the hydrogen pressure reaches 1000 psi (6.9 MPa). It should be noted that these results were based on notched tensile specimens. Therefore, the data may inadequate for stress analysis but can be used for comparison purposes. It is worth noting, however, Christenson et al. [10] did compare the fracture behavior and morphology from the two types of hydrogen charge (i.e., the cathodic charge in Figure 10 and the high pressure hydrogen atmosphere in Figure 11). They concluded that the qualitative correspondence between the hydrogen charge techniques could be established. For example, charging at 2.5 mA/cm² gave results similar to the testing in 3000 psi (21 MPa) hydrogen environment. The general observation remains the same, that is, the strength of the materials was not affected significantly by hydrogen, but the ductility was decreased as a result of hydrogen exposure.

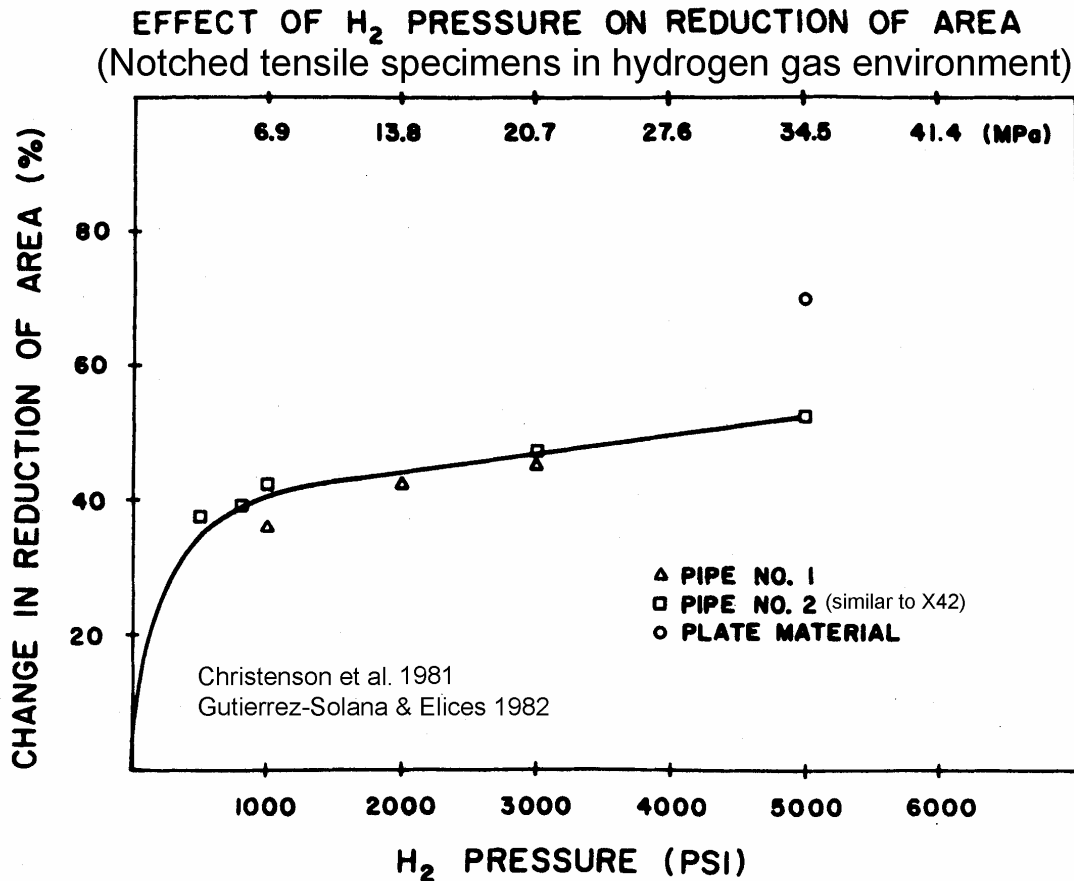


Figure 11 Change in reduction of area as a function of exposing hydrogen pressure for Spanish line pipe materials using double-notched tensile specimens [10,11].

The tensile properties obtained in 1000 psig (6.9 MPa) hydrogen environment for some API pipeline materials (X42 and X70) and low carbon steels (A516 and A106B) were reported by Cialone and Holbrook (1988) in Table 2 of Reference 12, and by Holbrook, Cialone, Mayfield, and Scott (1982) in Table 2 of 13, on their fatigue and subcritical crack growth studies. Because the tests were performed mainly within the same research group, their results are consolidated in Table 5. The carbon contents for these materials, X42, X70, A516, and A106B are, respectively, 0.26, 0.09, 0.21, and 0.26%. For manganese contents, they are, respectively, 0.82, 1.50, 1.04, and 0.57%. The API X-60 was also tested [13], but the properties in hydrogen were not reported. Therefore, the data for X60 are not included in this report.

Table 5 Tensile properties for X42, X70, A516, and A106B in air and in 1000 psi (6.9 MPa) hydrogen gas [12,13]

Steel	Test Environment	0.2% Offset Yield Stress MPa (ksi)	UTS MPa (ksi)	Elongation in 1 inch gage %	Reduction of Area %
X42 Longitudinal	Air	366 (53)	511 (74)	21	56
	6.9 MPa H ₂	331 (48)	483 (70)	20	44
X42 Transverse	Air	311 (45)	490 (71)	21	52
	6.9 MPa H ₂	338 (49)	476 (69)	19	41
X70 Longitudinal	Air	584 (85)	669 (97)	20	57
	6.9 MPa H ₂	548 (79)	659 (95)	20	47
X70 Transverse	Air	613 (89)	702 (102)	19	53
	6.9 MPa H ₂	593 (86)	686 (99)	15	38
A516	Air	372 (54)	538 (78)	17	70
	6.9 MPa H ₂	365 (53)	552 (80)	20	43
A106B	Air	462 (67)	558 (81)	14	58
	6.9 MPa H ₂	503 (73)	579 (84)	11	50

THRESHOLD STRESS INTENSITY FACTOR (K_{th} or K_H)

Longinow and Phelps (1975) [14] used wedge-opening-loaded (WOL) specimens to determine the critical stress intensity factor (K_H) at which the crack arrest occurred in specimens to hydrogen. The pre-cracked WOL specimens were loaded in air to 30 to 95% of the fracture toughness of the material in air, then exposed to 3000 to 14,000 psi (21 to 97 MPa) high purity hydrogen gas at ambient temperature. The stress intensity factor decreased as the crack propagation was initiated in hydrogen after an incubation time. As a result, K_H is defined as the lowest stress intensity factor achieved in the testing, below which the crack propagation in hydrogen is unlikely. The critical crack size can be estimated with fracture mechanics principle and the value of K_H .

Longinow and Phelps investigated various materials with a wide range of yield stress. When the values of K_H were averaged based on the yield stress, they found that the behavior of K_H seemed to form two separate groups: 1) steels with 85 to 113 ksi (586 to 779 MPa) yield stress and with 126 to 153 ksi (869 to 1055 MPa) yield stress. The results can be found in Reference 14 and are reproduced in Figure 12 of this report.

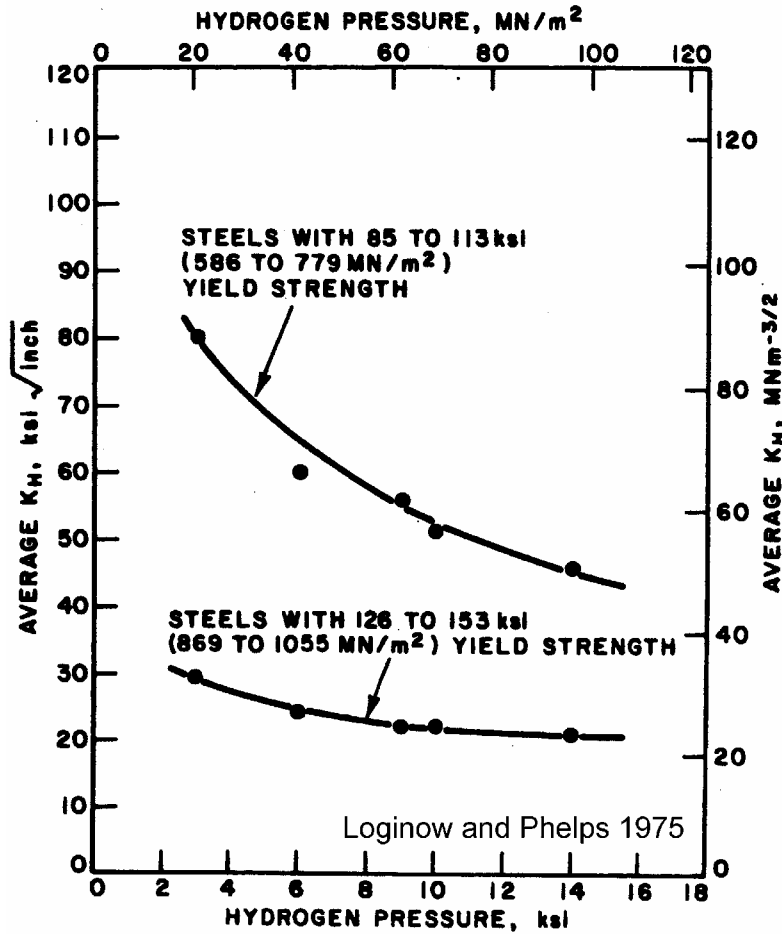


Figure 12 Threshold stress intensity factors at crack arrest in various hydrogen pressures [14].

Similarly, Cialone and Holbrook (1988) [12] performed subcritical crack growth experiments for X70 steel, X42 heat affected zone (HAZ), and a hardened X42 steel. The specimens were loaded in fixed displacement condition and tested in various pure gases and their mixtures with a total pressure of 6.9 MPa (1000 psi) regardless the gas compositions. The initial displacement was selected from the fracture toughness test data where the crack initiation was observed. Only hardened X42 exhibited crack growth in the mixture of 60% hydrogen and 40% methane (by volume) with total pressure of 6.9 MPa.

FRACTURE TOUGHNESS

Fracture toughness properties are reported in the literature typically in terms of K_{IC} (plane strain fracture toughness), J_{IC} (elastic-plastic fracture toughness in term of J-integral), crack growth resistance or J-R curve, and dJ/da which is the slope of the fracture resistance curve and is related to the tearing capability of the material. The representative results in the open literature for hydrogen-exposed carbon steel fracture properties are summarized in this section.

Robinson and Stoltz (1981) [15] used double-edged notched specimens of A516 Grade 70 (0.21% C, 1.04% Mn) for J-R curve testing in air and in hydrogen at pressures from 3.45 to 34.5 MPa (500 to 5000 psi). The test results are reproduced in Figure 13, from which they concluded that the hydrogen effect occurs at 3.45 MPa (due to fracture mode change) and is saturated at 34.5 MPa. In addition, the slope of the J-R curve (dJ/da , where J is the J-integral and a is the crack length) remains nearly constant regardless of the hydrogen pressure, indicating that hydrogen does not affect the ductile tearing through the pearlite colonies, while the crack initiation J_{IC} is related to the fracture of the ferrite that is controlled by the hydrogen-dislocation interaction. The numerical values of Figure 13 are tabulated in Table 6. Note that dJ/da is proportional to the Paris tearing modulus [16] which is related to the tearing capacity of the material.

The fracture toughness for A106 Grade B carbon steel was determined alternatively with information from burst tests conducted by Robinson and Stoltz [15]. A longitudinal, 20% part-through wall flaw was machined to each of the 10 cm diameter pipes. The test was performed with nitrogen gas and with 6.9 MPa hydrogen pressure plus overpressure nitrogen to burst. The estimated fracture toughness in the inert environment (nitrogen) is $K_{IC} = 114 \text{MPa}\sqrt{\text{m}}$ (104 $\text{ksi}\sqrt{\text{in}}$). Under 6.9 MPa hydrogen partial pressure, the burst test resulted in $K_{IC} = 85 \text{MPa}\sqrt{\text{m}}$ (77 $\text{ksi}\sqrt{\text{in}}$).

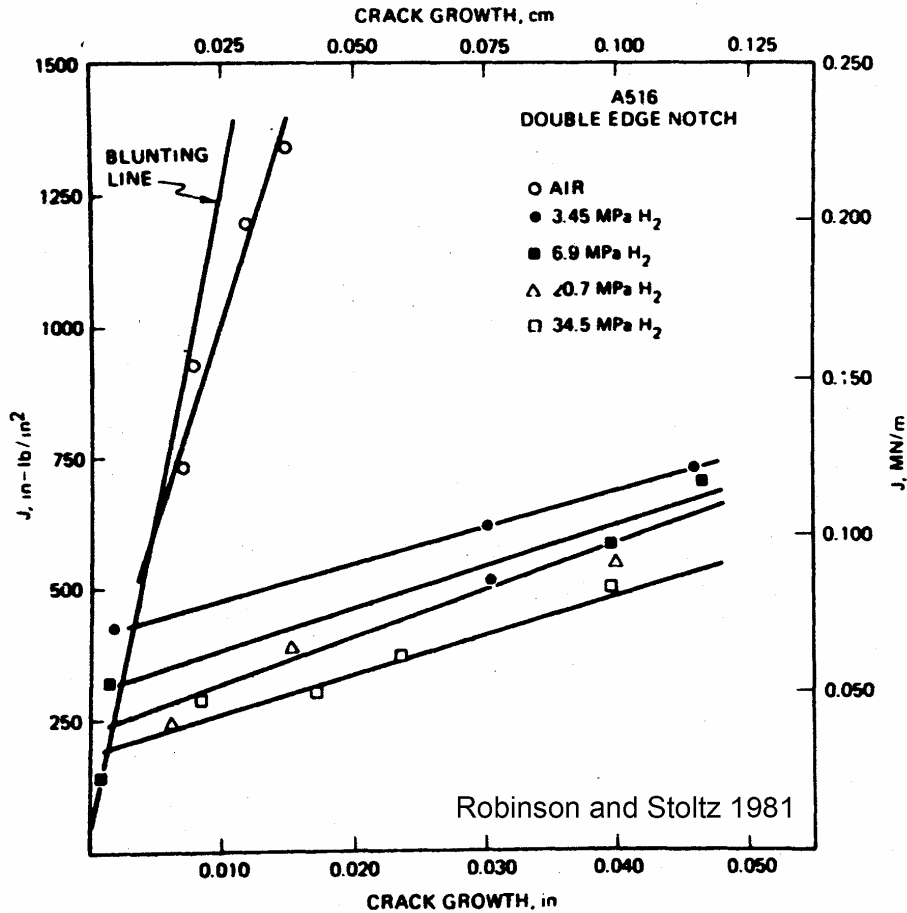


Figure 13 Crack growth resistance (J-R) curves for A516 Grade 70 in Air and in Hydrogen [15].

Table 6 Fracture toughness (J-R curve) for A516 Grade 70 in air and in hydrogen [15]

A516-70	J _{IC}			K _{IC}		dJ/da	
	MN/m	kJ/m ²	in-lb/in ²	MPa√m	ksi√in	MPa	lb/in ²
Air	0.121	121	697	150	137	516	7.5x10 ⁴
H ₂ 3.5 MPa	0.076	76	438	119	108	47	6.9x10 ³
H ₂ 6.9 MPa	0.056	56	322	102	93	55	8.1x10 ³
H ₂ 20.7 MPa	0.042	42	243	89	81	54	8.9x10 ³
H ₂ 34.5 MPa	0.036	36	207	82	75	57	8.3x10 ³

Gutierrez-Solana and Elices [11] performed fracture toughness testing for a Spanish transmission pipeline material similar to X42 steel under hydrogen pressure. The three-point bend test was conducted in high pressure chamber with high purity hydrogen up to 6.5 MPa. The finite element analysis was used to verify the experimentally obtained J-integral values. In addition, burst tests were carried out for pipes with various

configurations of longitudinal machined cracks. Similar to Robinson and Stoltz [15], the fracture toughness was estimated from the burst test data. The burst test specimens were allowed sufficient time in the hydrogen environment to achieve maximum embrittlement then pressurized to burst. The highest hydrogen pressure recorded was 16 MPa. The plane strain fracture toughness, K_{IC} , were calculated with analytical solution and plotted collectively with the three-point bend data in Figure 14. The numerical data are shown in Table 7 for the three-point bend test, and in Table 8 for the burst test. Note that the actual burst pressure was slightly higher than the hydrogen pressure for each test.

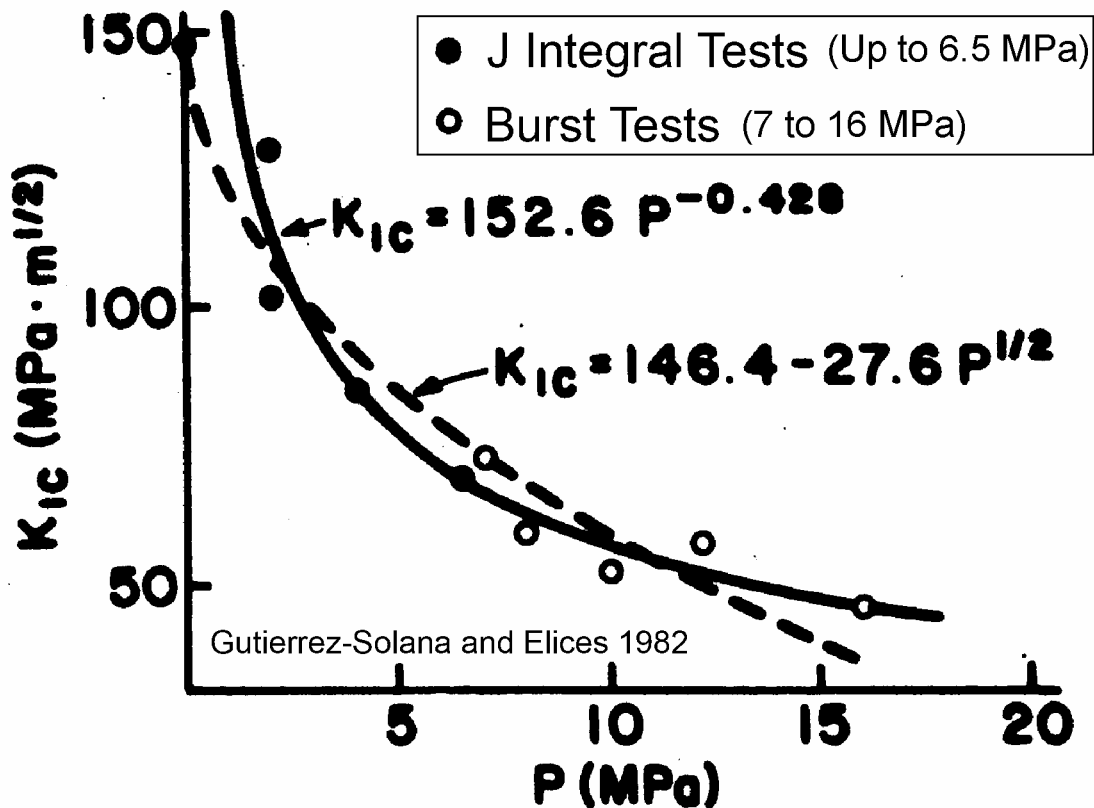


Figure 14 Hydrogen pressure-dependent fracture toughness for a Spanish line pipe material similar to API X42 [11].

Table 7 Three-point bend fracture toughness test results for a Spanish line pipe material similar to API X42 under hydrogen pressure (see Figure 14) [11]

H ₂ Pressure (MPa)	J _{IC} (kJ/m ²)	K _{IC} (MPa√m)	dJ/da (MPa)	δ _c ^{**} (mm)
0	99.8±3.8	147	111	0.134
2	76 / 48	128 / 101	NA	NA
4	33.3±2.1	85	36	0.035
6.5	22.3±2.1	69	31	0.029

** δ_c is the critical crack tip opening displacement (CTOD), obtained from crack mouth opening displacement (CMOD) measured when J= J_{IC}.

Table 8 Fracture toughness data determined by burst test for a Spanish line pipe material similar to API X42 under hydrogen pressure (see Figure 14) [11]

H ₂ Pressure (MPa)	Burst Pressure (MPa)	K _{IC} (MPa√m)
7	9.4	73
8	8.4	59
10	11.1	53
12.2	15.8	57
16.0	16.8	46

Fracture testing for J-R curves was reported by Cialone and Holbrook (1988) [12] for X42 and X70 under various gas condition with total pressure of 6.9 MPa independent of the composition of the gas mixtures. Figure 15 shows the comparison of the J-R curves for X42 in 6.7 MPa (1000 psig) pressure of nitrogen (inert condition) and in 6.7 MPa (1000 psig) hydrogen, respectively. The numerical values for crack initiation (J_{IC}) and for the slope of the J-R curves (dJ/da) representing the tearing capability of the material [16] are listed in Table 9, from which the only significant reduction in dJ/da can be seen in the case of X70.

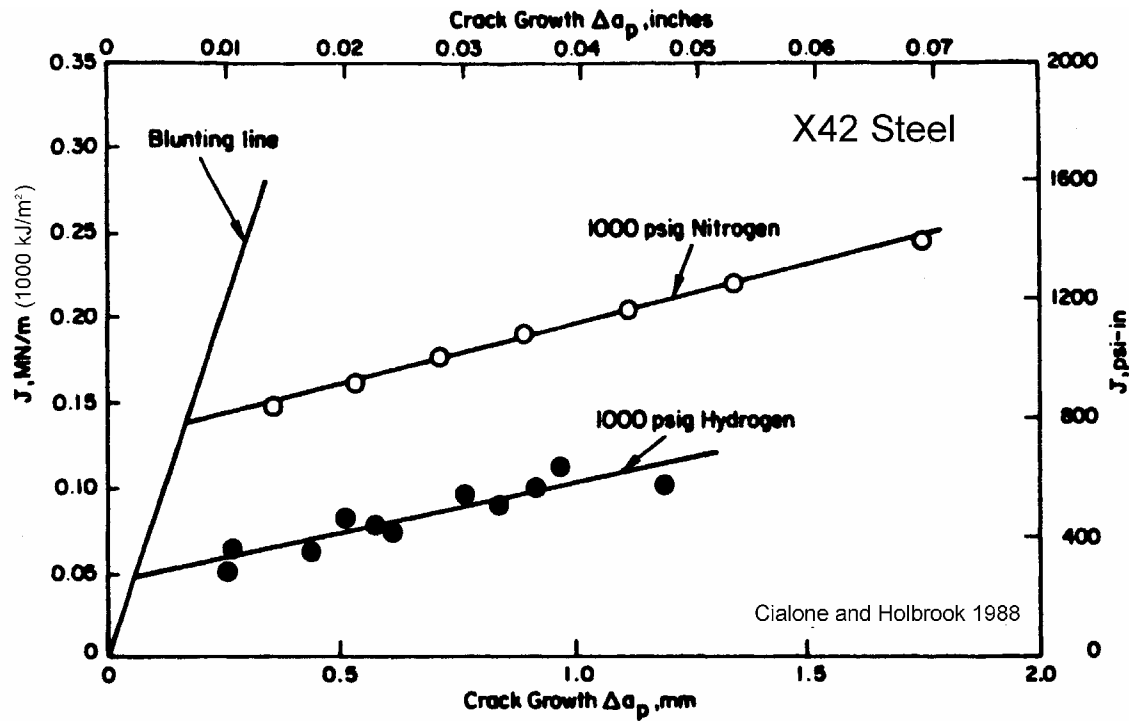


Figure 15 The crack growth resistance (J-R) curves for X42 base metal in 6.9 MPa (1000 psig) pressure of nitrogen and in 6.9 MPa of hydrogen [12].

Table 9 Fracture toughness (J_{IC} and dJ/da) for X42 and X70 in 6.9 MPa nitrogen and in 6.9 MPa hydrogen [12]

Material	J_{IC} (MN/m)		dJ/da (MPa or MN/m ²)	
	N ₂ 6.9 MPa	H ₂ 6.9 MPa	N ₂ 6.9 MPa	H ₂ 6.9 MPa
X42	0.14	0.05	70	63
X70	0.17	0.04	251	23
X42 HAZ	0.02	0.01	97	69

Recently, Charpy V-notch impact tests, elastic-plastic fracture toughness tests, and constant load fatigue tests were carried out by Zawierucha and Xu (2005) [17] using API 5L Grade B steel. This steel received multiple certifications as API 5L Product Specification Level (PSL) 1 Grade B [1], ASTM A53 Grade B, ASME SA53 Grade B, ASTM A106 Grade B/C, and ASMESA-106 Grade B/C. The carbon and manganese contents are respectively 0.18 and 1.06%, with carbon equivalent[†] (CE) 0.37. It was tested as rolled and normalized (900 °C for one hour followed by air cool) conditions. The normalization increases the 0.2% Young’s modulus, UTS, elongation, and reduction of area from 299 MPa, 518 MPa, 28%, and 54.9%, respectively, to 371 MPa, 539 MPa, 32.9%, and 61%.

[†] For carbon content greater than 0.12%, API 5L [1] specifies that $CE=C + Mn/6 + (Cr + Mo + V)/5 + (Ni + Cu)/15$

Typically, the effects of hydrogen on the J-R curve for API 5L Grade B can be seen in Figure 16, where the compact tension specimens were tested in 13.8 MPa (2000 psi) nitrogen and in 13.8 MPa (2000 psi) hydrogen, respectively. The complete results of fracture toughness testing can be found in Table 10. The J_{IC} data in Table 10 are plotted in Figure 17. Note that the specimen tested in 13.8 MPa nitrogen did not meet the J_{IC} requirement specified by ASTM E 1820 [18]. Therefore, the fracture toughness was obtained by correlating the Charpy impact test results [19]. The estimated K_{IC} for the as rolled materials is $120 \text{ MPa}\sqrt{\text{m}}$ (in nitrogen with 13.8 MPa), and the equivalent J_{IC} is 70 kJ/m^2 .

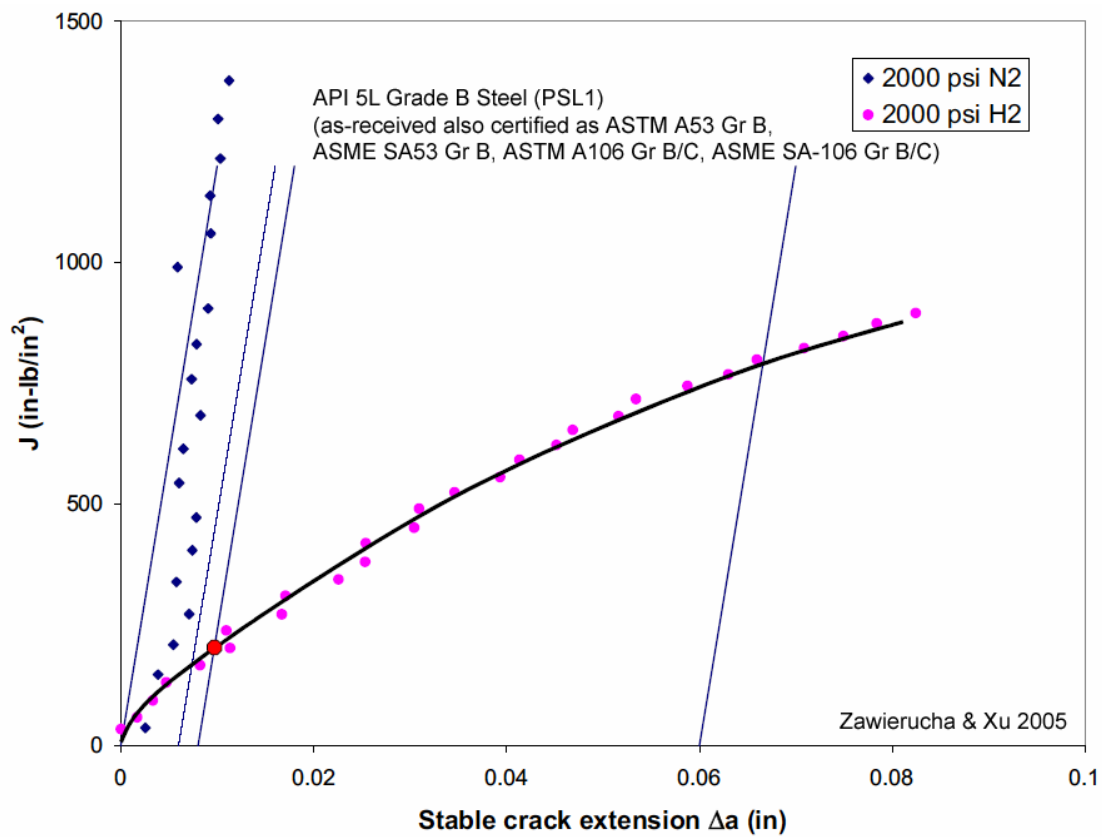


Figure 16 The J-R curves for API 5L Grade B in 13.8 MPa (2000 psi) nitrogen and in 13.8 MPa (2000 psi) hydrogen [17].

Table 10 Fracture toughness for API 5L Grade B exposed to various pressures of hydrogen [17]

Material	H ₂ Pressure		Loading Rate mm/min	J _{IC}		K _{JC}	
	MPa	psi		kJ/m ²	in-lb/in ²	MPa√m	ksi√in
As rolled	13.8	2000	0.5	33.8	193	84	76
As rolled	3.5	500	0.05	42.2	241	94	86
As rolled	6.9	1000	0.05	38.0	217	89	81
As rolled	13.8	2000	0.05	32.0	183	81	74
As rolled	20.7	3000	0.05	33.3	190	83	76
Girth Weld	13.8	2000	0.05	59.5	340	111	101
Girth HAZ	13.8	2000	0.05	39.9	228	91	83
Normalized	3.5	500	0.05	49.2	281	101	92
Normalized	5.2	750	0.05	43.4	248	95	86
Normalized	6.9	1000	0.05	42.7	244	95	86
Normalized	13.8	2000	0.05	36.1	206	87	79

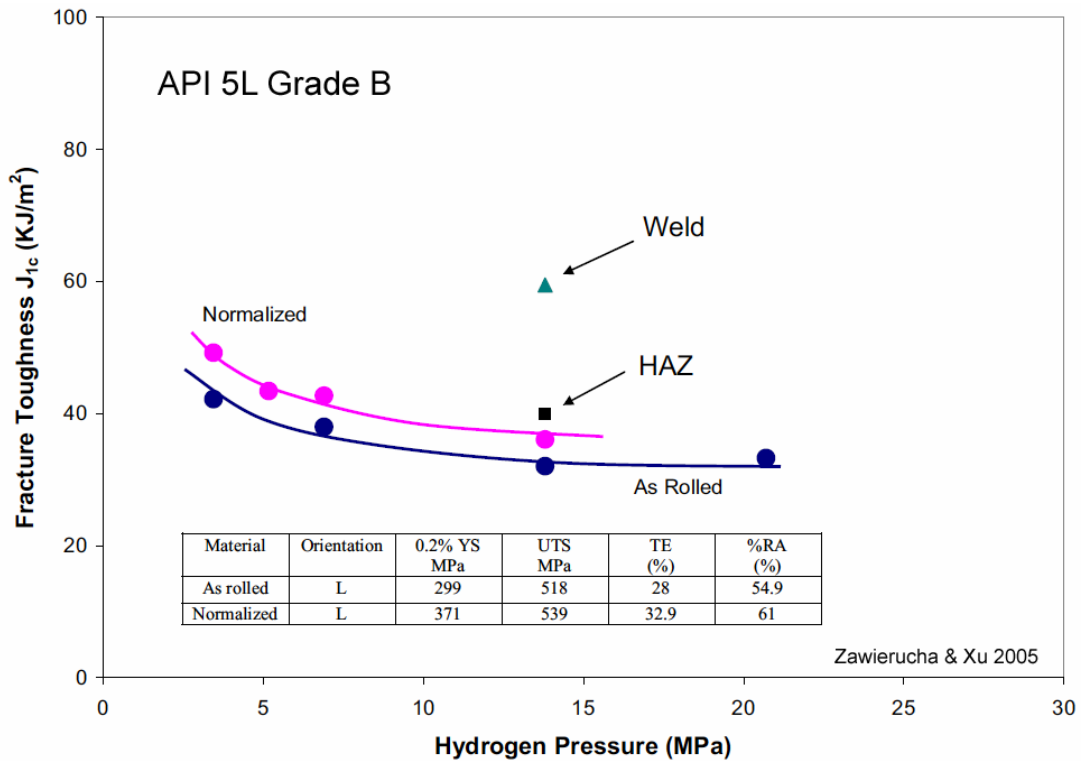


Figure 17 The pressure dependent J_{IC} for API 5L Grade B in hydrogen [17]

FATIGUE CRACK GROWTH

The fatigue crack growth rate (i.e., da/dN) of materials is a function of the maximum stress (K_{max}), minimum stress (K_{min}), stress range ($\Delta K = K_{max} - K_{min}$), stress ratio ($R = K_{min}/K_{max}$), and cyclic frequency. Because vast amount of data exist in the open literature for carbon steels, only typical results of fatigue testing in pressurized hydrogen gas environment for API 5L line pipe materials with moderate strength [12,17], and for ASME SA-105 Grade II steel [20], are reported in this section of the report.

The API X42 and X70 line pipe steels were used by Cialone and Holbrook (1988) [12] in a comprehensive hydrogen test program including the tensile, subcritical crack growth, and fracture tests which have documented in previous sections. Some of their fatigue test data of fatigue crack growth rate tests are shown in Figure 18, from which the fatigue crack growth rates in 6.9 MPa (1000 psig) hydrogen and in 6.9 MPa (1000 psig) can be compared. In these two cases, low stress ratio ($R = 0.1$) were used in testing. It can be seen that da/dN appears to be higher in X42 steel than in X70 at the same ΔK level. In the case of X42, the fatigue crack growth rate can be 150 times greater than that in the nitrogen, under the same 6.9 MPa pressure. The tests were also carried out at higher stress ratios (R ranges from 0.1 to 0.8). These results for X42 are summarized in Figure 19.

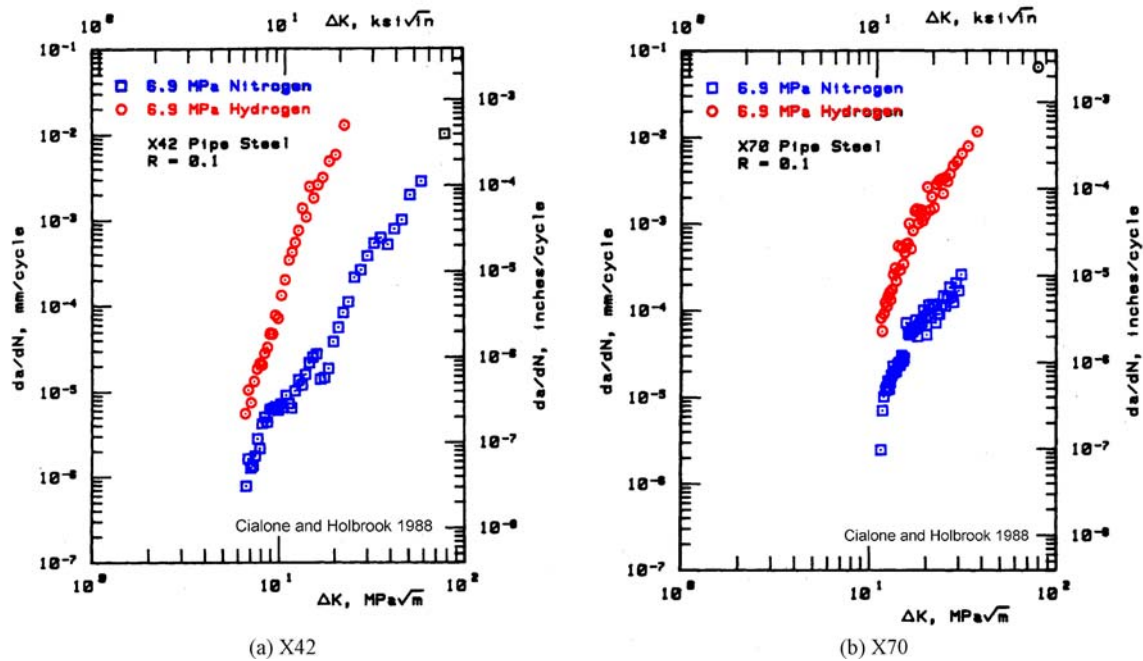


Figure 18 Fatigue crack growth rates (da/dN) for (a) X42 and (b) X70 in 6.9 MPa (1000 psi) hydrogen and in 6.9 MPa (1000 psi) nitrogen at stress ratio $R = 0.1$ [12]

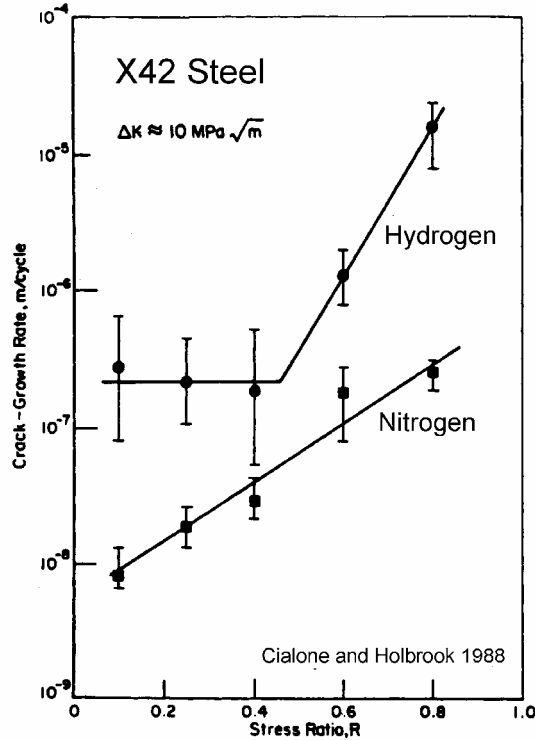


Figure 19 Fatigue crack growth rates (da/dN) for X42 in hydrogen and in nitrogen at various stress ratios (R) [12].

The fracture toughness of the as-rolled and normalized API 5L Grade B line pipe steel obtained by Zawierucha and Xu (2005) [17] was reported in the previous section. The corresponding fatigue crack growth rates with stress ratio $R=0.1$ under 1.4 and 20.7 MPa hydrogen pressures are shown in Figure 20. It can be concluded that the presence of hydrogen significantly increased the fatigue crack growth rate of the material (20 to 50 times higher than in the air). In addition, over the tested ΔK range ($16.5 < \Delta K < 25.3 \text{ MPa}\sqrt{\text{m}}$), the fatigue crack growth rate seemed insensitive to the pressure of hydrogen (i.e., da/dN only increased about 1.5 times when the hydrogen pressure changed from 1.4 MPa to 20.7 MPa). Additional hydrogen pressures were applied in the fatigue crack growth tests. Figure 21 shows the dependence of fatigue crack growth rate on the hydrogen pressure when $\Delta K=22 \text{ MPa}\sqrt{\text{m}}$. The heat treatment used to normalize the as-rolled material did not affect the fracture toughness and the fatigue crack growth rate of the material. Note that the tensile property change due to the heat treatment can be seen in the inset of Figure 17.

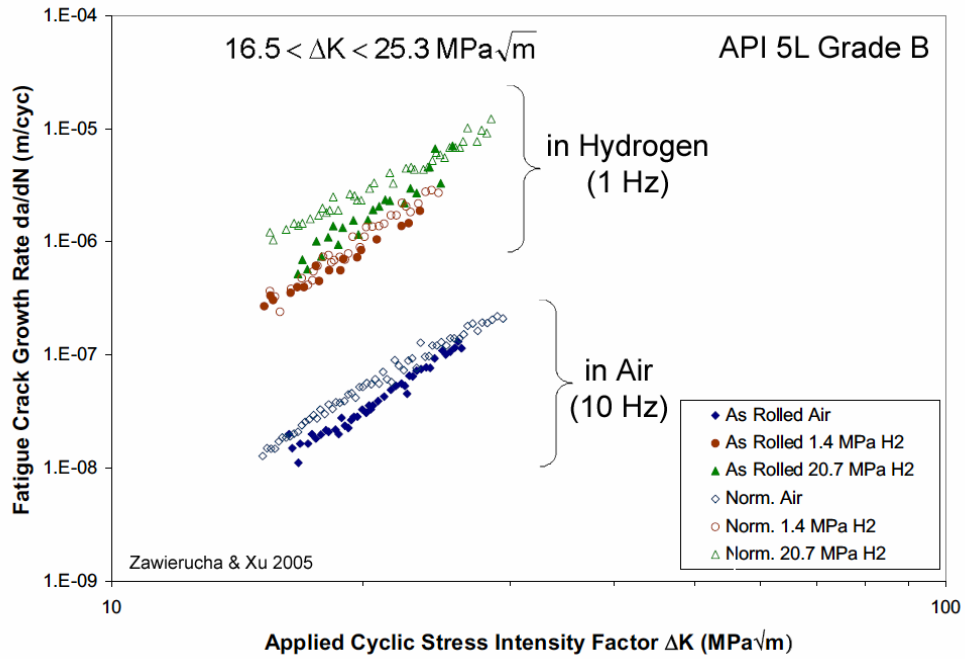


Figure 20 Fatigue crack growth rates (da/dN) for as rolled and normalized API 5L Grade B steels in various pressures of hydrogen (1Hz) and in air (10 Hz) [17].

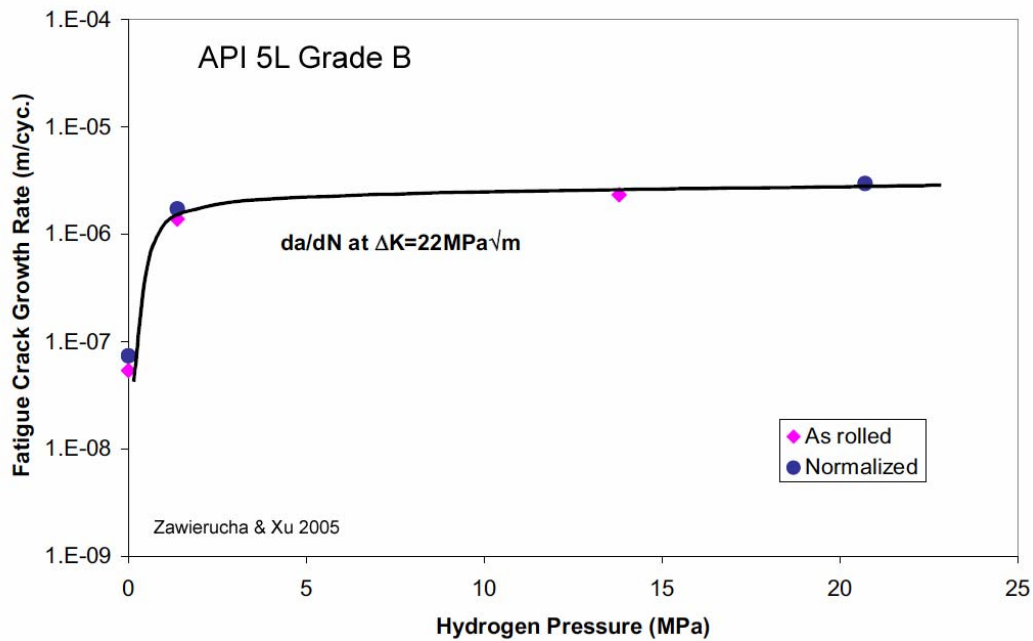


Figure 21 Fatigue crack growth rates (da/dN) for as rolled and normalized API 5L Grade B steels as a function of hydrogen pressure [17]

An extensive investigation of fatigue properties was conducted by Walter and Chandler (1976) [20] for ASME SA-105 Grade II steel (0.23% C and 0.62% Mn) used in high-pressure hydrogen compressor systems. Tapered, double-cantilever beam (TDCB) specimens were instrumented and tested in high purity hydrogen up to 103.4 MPa (15,000 psi) at ambient temperature (70 °F). The dependence of fatigue crack growth rate (da/dN) on the hydrogen pressure (6.9, 68.9, and 103.4 MPa or 1000, 10,000, and 15,000 psi) is shown in Figure 22. The test data of companion specimens in helium are also included for comparison. It can be seen that the crack growth rate is strongly affected by the presence of hydrogen. However, da/dN is approximately the same in different hydrogen pressures when ΔK is greater than $33\text{MPa}\sqrt{\text{m}}$ ($30\text{ksi}\sqrt{\text{in}}$). This behavior is consistent with the results in Figure 21 (Zawierucha and Xu [17]).

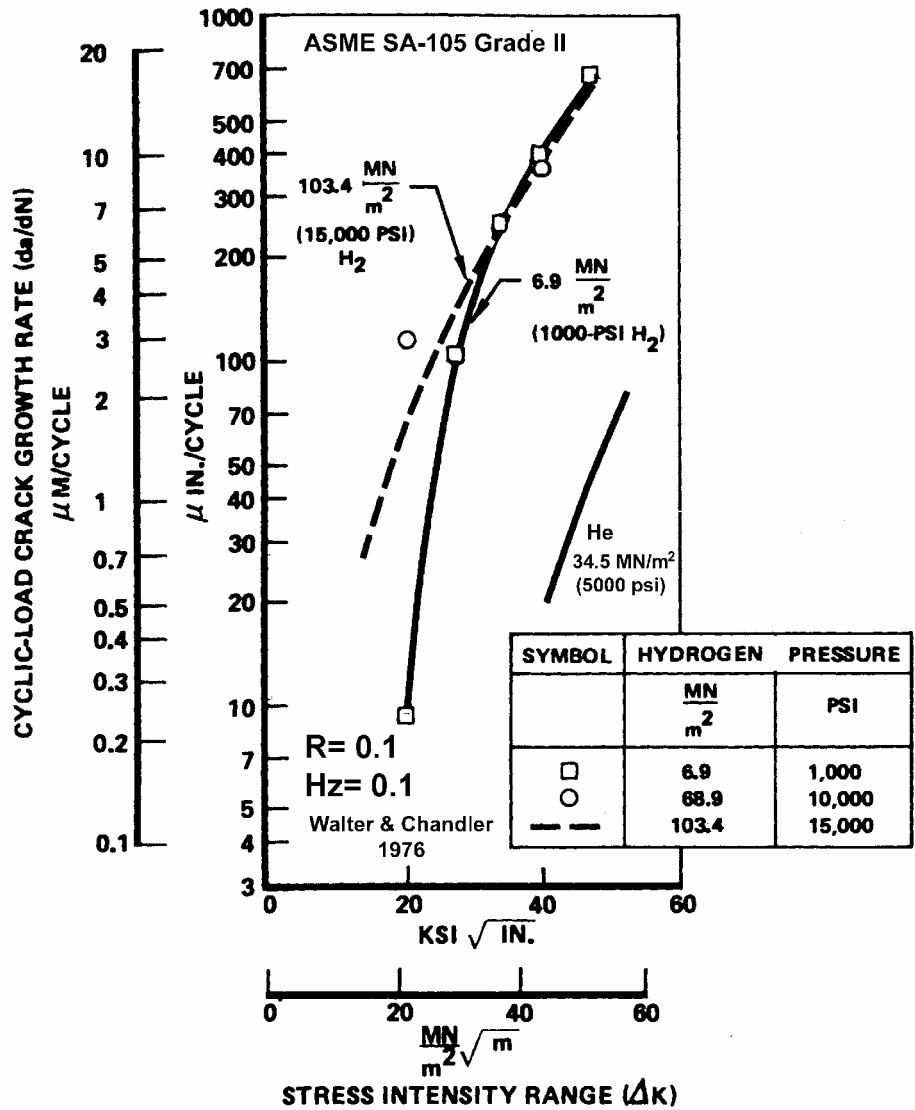


Figure 22 Fatigue crack growth rate for ASME SA-105 Grade II steel exposed to hydrogen up to 15,000 psi under R=0.1 and 0.1 Hz cyclic load [20]

Figure 23 shows the response of da/dN as a function of ΔK under various loading frequencies for ASME SA-105 Grade II steel in hydrogen. The test data in helium are included for comparison.

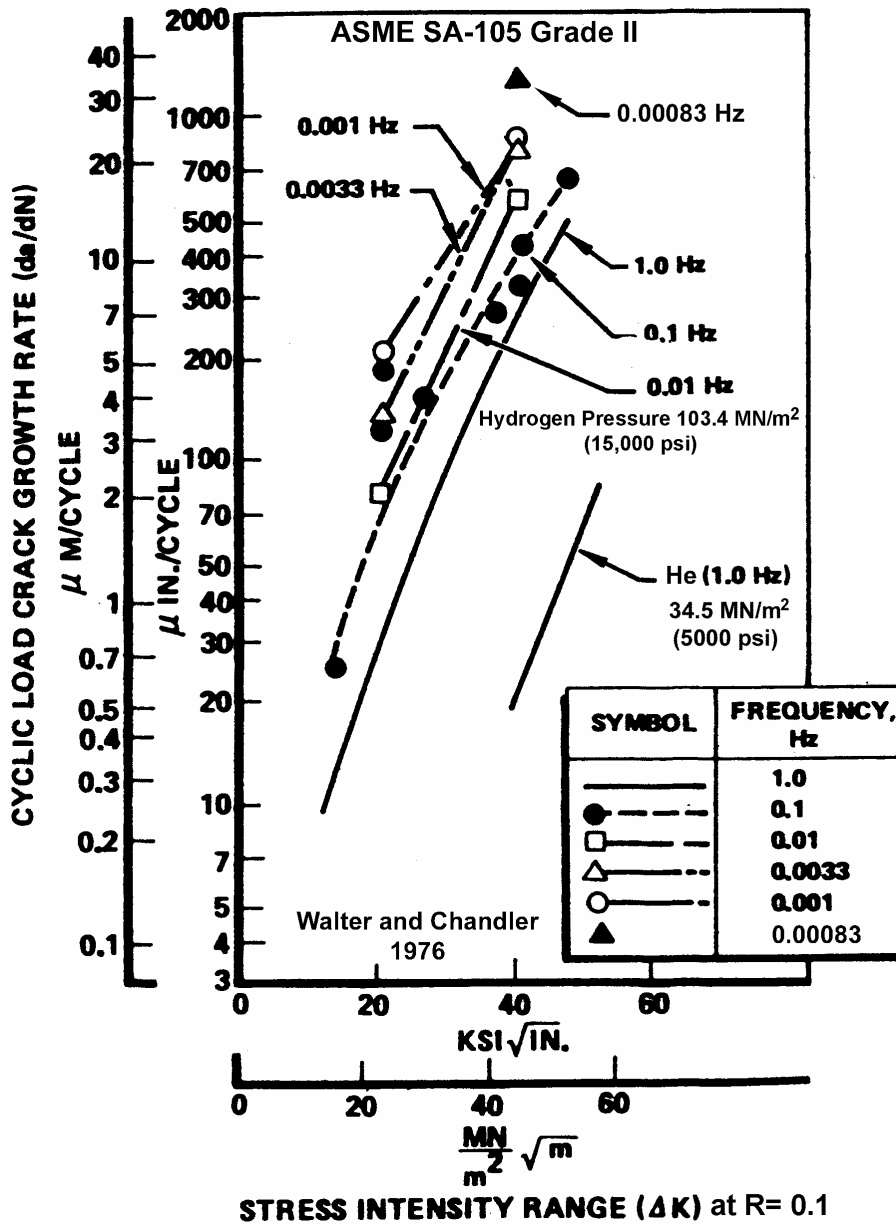


Figure 23 Cyclic frequency effects on ASME SA-105 Grade II steel in 15,000 psi hydrogen (R= 0.1) [20]

The effects of stress ratio were also investigated by these authors [20]. They varied the stress ratios (R) with a fixed K_{max} in one group of tests, and used a constant R= 0.1 but

varied K_{\max} in another group. The K_{\max} used in this study was below $50 \text{ MPa}\sqrt{\text{m}}$, which is about one-half of the typical K_{IC} for ASME SA-105 Grade II steel (generally greater than $100 \text{ MPa}\sqrt{\text{m}}$ or $91 \text{ ksi}\sqrt{\text{in}}$). The test data of Walter and Chandler [20] were shown to fall on a curve which can be defined by a simple Paris power law [21,22] as a function of ΔK only (unless K_{\max} approaches the stress intensity factor for unstable crack growth). This implies that da/dN strongly depends on the stress range (or ΔK), and a high K_{\max} does not significantly affect the fatigue crack growth for this material. Note that Cialone and Holbrook [12] showed the dependence of da/dN on R (Figure 19) for X42 steel.

In general, a tensile overload in fatigue testing causes a retardation in crack propagation because of a plastic wake occurs behind the crack tip [23]. Walter and Chandler (1976) [20] reported that a preloading (overload) in air to a stress intensity factor 1.5 times the cyclic K_{\max} did not seem to affect da/dN in 103.4 MPa (15,000 psi) hydrogen for ASME SA-105 Grade II steel, while the same preloading indeed retarded the subsequent fatigue crack growth when the test was carried out in 34.5 MPa (5000 psi) helium. It appears that the hydrogen embrittlement diminished the plasticity effect in this steel.

CONCLUSIONS

Tensile properties (yield stress, ultimate tensile stress, elongation, and reduction of area), threshold stress intensity factor (or the critical stress intensity factor at crack arrest), fracture toughness (J-R curve, J_{IC} , or K_{IC}), and the fatigue crack growth rate (da/dN) which were reported in the open literature for low carbon steel and line pipe steels with up to moderate strengths in the gaseous hydrogen environment have been summarized in this report. In general, the hydrogen pressure does not have pronounced effects on the yield stress and the UTS. In addition, the hydrogen pressure would either increase or decrease the yield stress and the strain hardening behavior. However, hydrogen has a significant effect on decreasing the ductility of the material (i.e., the elongation and the reduction of area). It was also demonstrated by all the investigators that the hydrogen pressure will significantly reduce the fracture toughness (both initiation and dJ/da or tearing capacity) and accelerate the fatigue growth rate.

The hydrogen effects on these mechanical properties of the carbon steel and the pipeline materials depend on many factors such as the pressure and purity of the hydrogen gas, the loading range and loading rate. As a result, the concept of a composite plot to show all the available literature data for comparison purpose would not be possible. However, the collection of literature data is by no means complete, but the diversity of data and dependency of results in test method is sufficient to warrant a design and implementation of a thorough test program. The program would be needed to enable a defensible demonstration of structural integrity of a pressurized hydrogen system. It is essential that the environmental variables be well-defined (e.g., the applicable hydrogen gas pressure range and the test strain rate) and the specimen preparation be realistically consistent (such as the techniques to charge hydrogen and to maintain the hydrogen concentration in the specimens). To facilitate the predictive methodology and the fitness-for-service

assessment analyses, the companion tensile testing for the full stress-strain curve should be performed along with the fracture and fatigue tests, which are expected to be an integral part of code and standard development for hydrogen services.

REFERENCES

- 1 *Specification for Line Pipe*, API Specification 5L, 43rd Edition, March 2004, American Petroleum Institute, Washington, DC.
- 2 Kimura, H., Matsui, H., Kimura, A., Kimura, T., and Oguri, K., 1981, "Softening and Hardening in High Purity Iron and Its Alloys Charged with Hydrogen," *Hydrogen Effects in Metals*, ed. I. M. Bernstein and A. W. Thompson, The Metallurgical Society of American Institute of Mining, Metallurgical, and Petroleum Engineers (AIME), Inc., New York, NY, pp. 191-208.
- 3 Jewett, R. P., Walter, R. J., Chandler, W. T., and Frohberg, R. P., 1973, *Hydrogen Environment Embrittlement of Metals*, prepared by Rocketdyne, Division of North American Rockwell, Canoga Park, CA. for National Aeronautics and Space Administration, Washington, DC, NASA Contractor Report NASA CR-2163.
- 4 Hofmann, W. and Rauls, W., 1961, *Archiv für das Eisenhüttenwesen*, p. 1.
- 5 Hofmann, W. and Rauls, W., 1962, *Dechema Monograph*, 45, p. 33.
- 6 Hofmann, W. and Rauls, W., 1965, *Welding J.*, p. 225-S.
- 7 Walter, R. J. and Chandler, W. T., *Effects of High-pressure Hydrogen on Metals at Ambient Temperature, Final Report*, Contract NAS8-19, NASA, MSFC, Huntsville, Alabama, Rocketdyne, a division of North American Rockwell Corp., Canoga Park, CA., Report R-7780-1,2, 3. Available through U. S. Department of Commerce, National Technical Information Service, N70-18637.
- 8 Ellis, M. B. D., Bartlett, R. A., and Knott, J. F., "Effects of Prestrain and Dissolved Hydrogen on the Tensile Properties and the Fracture Behavior of Line-Pipe Steels," 1990, *Hydrogen Effects on Material Behavior*, ed. N. R. Moody and A. W. Thompson, The Minerals, Metals, and Materials Society, Warrendale, PA, pp. 991-1002.
- 9 Pussegoda, L. N. and Tyson, W. R., 1981, "Relationship between Microstructure and Hydrogen Susceptibility of Some Low Carbon Steels," *Hydrogen Effects in Metals*, ed. I. M. Bernstein and A. W. Thompson, The Metallurgical Society of American Institute of Mining, Metallurgical, and Petroleum Engineers (AIME), Inc., New York, NY, pp. 349-360.
- 10 Christenson, D. J., Berstein, I. M., Thompson, A. W., Danielson, E. J., Elices, M., and Gutierrez-Solana, F., 1981, "Hydrogen Compatibility of a Line Pipe Steel," *Hydrogen Effects in Metals*, ed. I. M. Bernstein and A. W. Thompson, The Metallurgical Society of American Institute of Mining, Metallurgical, and Petroleum Engineers (AIME), Inc., New York, NY, pp. 997-1004.
- 11 Gutierrez-Solana, F. and Elices, M., 1982, "High-Pressure Hydrogen Behavior of a Pipeline Steel," *Current Solutions to Hydrogen Problems in Steels*, ed. C. G. Interrante and G. M. Pressouyre, American Society for Metals, Metals Park, OH, pp. 181-185.

- 12 Cialone, H. J. and Holbrook, J. H., 1988, "Sensitivity of Steels to Degradation in Gaseous Hydrogen," *Hydrogen Embrittlement: Prevention and Control*, ASTM STP 962, ed. L. Raymond, American Society for Testing and Materials, Philadelphia, pp. 134-152.
- 13 Holbrook, J. H., Cialone, H. J., Mayfield, M. E., and Scott, P. M., 1982, *The Effect of Hydrogen on Low-Cycle-Fatigue and Subcritical Crack Growth in Pipeline Steels*, Battelle Columbus Laboratories, Columbus, Ohio, available through U. S. Department of Commerce, National Technical Information Service, DE85006685.
- 14 Loginow, A. W. and Phelps, E. H., 1975, "Steels for Seamless Hydrogen Pressure Vessels," *Corrosion*, 31(11), pp. 404-412.
- 15 Robinson, S. L. and Stoltz, R. E., 1981, "Toughness Losses and Fracture Behavior of Low Strength Carbon-Manganese Steel in Hydrogen", *Hydrogen Effects in Metals*, ed. I. M. Bernstein and A. W. Thompson, The Metallurgical Society of American Institute of Mining, Metallurgical, and Petroleum Engineers (AIME), Inc., New York, NY, pp. 987-993
- 16 Paris, P. C., Tada, H., Zahoor, A., and Ernst, H., 1979, "The Theory of Instability of the Tearing Mode of Elastic-plastic Crack Growth," *Elastic-Plastic Fracture*, ASTM STP 668, J. D. Landes, J. A. Begley, and G. A. Clarke, eds., American Society for Testing and Materials, pp. 5-36.
- 17 Zawierucha, R. and Xu, K., 2005, "Hydrogen Pipeline Steels," *Materials Science & Technology - Materials for the Hydrogen Economy*, organized by J. J. Petrovic, I. E. Anderson, T. M. Adams, G. Sandrock, C.F. Legzdins, J.W. Stevenson, and Z.G. Yang, 2005; *Materials Science & Technology 2005*, pp. 79-90.
- 18 ASTM E 1820, *Standard Test Method for Measurement of Fracture Toughness*, American Society for Testing and Materials.
- 19 Barsom, J. M. and Rolfe, S., 1999, *Fracture and Fatigue Control in Structures: Applications of Fracture Mechanics*, 3rd Edition, American Society for Testing and Materials, p. 119.
- 20 Walter, R. J. and Chandler, W. T., 1976, "Cyclic-load Crack Growth in ASME SA-105 Grade II Steel in High-pressure Hydrogen at Ambient Temperature," *Effect of Hydrogen on Behavior of Materials*, ed. A. W. Thompson and I. M. Bernstein, The Metallurgical Society of American Institute of Mining, Metallurgical, and Petroleum Engineers (AIME), Inc., New York, NY, pp. 273-286.
- 21 Paris, P. C., Gomez, M. P., Anderson, W. P., 1961, "A Rational Analytic Theory of Fatigue," *The Trend in Engineering*, Vol. 13, pp. 9-14.
- 22 Paris, P. C. and Erdogan, F., 1960, "A Critical Analysis of Crack propagation Laws," *Journal of Basic Engineering*, Vol. 85, pp. 528-534.
- 23 Elber, W., 1971, "The Significance of Fatigue Crack Closure," *Damage Tolerance in Aircraft Structures*, ASTM STP 486, American Society for Testing and Materials, Philadelphia, pp. 230-242.

REPORT WSRC-TR-2006-00119 Rev. 1

DISTRIBUTION

SAVANNAH RIVER SITE

N. C. Iyer, 773-41A
R. L. Sindelar, 773-41A
T. M. Adams, 773-41A
A. J. Duncan, 773-A
G. B. Rawls, 773-41A
E. A. Clark, 773-A
E. W. Holtzscheiter, Jr., 773-A
T. Motyka, 773-41A
M. J. Morgan, 773-A
P. S. Lam, 773-41A

EXTERNAL

L. J. Eslin, Concurrent Technologies Corporation
F. R. Dax, Concurrent Technologies Corporation